



Minerva Access is the Institutional Repository of The University of Melbourne

Author/s:

Bhattacharyya, S;Sreekesh, S;King, A

Title:

Characteristics of extreme rainfall in different gridded datasets over India during 1983-2015

Date:

2022-04-01

Citation:

Bhattacharyya, S., Sreekesh, S. & King, A. (2022). Characteristics of extreme rainfall in different gridded datasets over India during 1983-2015. *Atmospheric Research*, 267, <https://doi.org/10.1016/j.atmosres.2021.105930>.

Persistent Link:

<https://hdl.handle.net/11343/332393>

1 Characteristics of extreme rainfall in different gridded datasets over
2 India during 1983-2015

3

4 Suman Bhattacharyya¹, S. Sreekesh^{1*} and Andrew King²

5 ¹Centre for the Study of Regional Development, Jawaharlal Nehru University, New Delhi,
6 India.

7 ²School of Earth Sciences and ARC Centre of Excellence for Climate Extremes, The
8 University of Melbourne, Melbourne, Australia.

9

10

11 * Corresponding author

12 Email: sreekesh@mail.jnu.ac.in

13

14

15

16

17

18

19

20

21

22

23

1 **Abstract**

2 Understanding the spatial and temporal occurrences of extreme rainfall events and their
3 changes is crucial for reducing the risk associated with extreme events, especially under
4 anthropogenic warming. This study presents a comparative analysis of twelve gridded
5 rainfall datasets in representing the spatial and temporal variation of extreme rainfall
6 events and trends in the recent past (1983 -2015) over India. The selected datasets fall into
7 four categories: gauge-based (APHRODITE, CPC, GPCC, REGEN), satellite-derived
8 (CHIRPS, PERSIANN-CDR), reanalysis (ERA-5, MERRA2, PGF, and JRA-55), and
9 products merged from these three types (WFDEI and MSWEP). For comparison, a gauge-
10 based, high resolution ($0.25^\circ \times 0.25^\circ$) daily gridded rainfall dataset, prepared by the India
11 Meteorological Department (IMD) is used as a reference dataset. Eleven extreme climate
12 indices, defined by the World Meteorological Organization's Expert Team on Climate
13 Change Detection and Indices (ETCCDI) and the IMD are used to represent the magnitude,
14 frequency, and duration of extreme rainfall events in India. The relative performance of
15 these datasets in capturing extreme rainfall events is evaluated by computing model
16 evaluation matrices i.e. correlation-coefficient (CC) and Percentage Bias (PBIAS). Trends in
17 extreme rainfall indices and their magnitudes are calculated using Mann-Kendell and Sen's
18 slope methods respectively, to compare with the IMD dataset. Our study finds large
19 uncertainties in representing extreme rainfall events where in most cases the datasets
20 underestimate higher extreme events compared to the IMD data. GPCC and MSWEP
21 better capture the magnitude, duration, and frequency of extreme rainfall events in India
22 and are comparable to the pattern of the IMD dataset. CHIRPS and ERA-5 perform better
23 than other satellite and reanalysis rainfall datasets. All of these selected datasets
24 consistently underestimate extreme rainfall events over the northern Himalayan region.
25 The gridded datasets are unable to capture the spatial pattern of observed trends in
26 extreme rainfall indices in India when compared t the IMD dataset.

27

28 *Keywords:* Extreme rainfall; Gridded rainfall dataset; ETCCDI extreme precipitation
29 indices; Reanalysis dataset; Merged dataset; Trend analysis.

30

1 **1. Introduction**

2 The nature of extreme climatic events, such as extreme rainfall, drought, and heat waves,
3 is changing as a consequence to recent human-induced warming (Fischer and Knutti et al.,
4 2015; Matthews et al., 2019; Perkins-Kirkpatrick and Lewis 2020;). Rainfall extremes have
5 socio-economic impacts as they often translate into devastating floods and droughts, which
6 hinder agricultural production and result in human casualties. Accurate measurements of
7 rainfall over the globe are crucial to understand rainfall processes, extremes, and their
8 changes associated with climate change. Point-based measurements of rainfall are highly
9 accurate, but are limited over the globe owing to the sparse distribution of gauge networks
10 (Kidd et al., 2017) and can suffer from data quality issues (Viney and Bates 2004). These
11 problems can be partly addressed by developing gridded rainfall datasets through the
12 interpolation of gauge-based rainfall data over regular grid surface. Various gridded
13 rainfall datasets are now available with global or near-global coverage but the relative
14 performance of these datasets varies in space and time (Sun et al., 2018). Despite several
15 limitations, gridded datasets are widely used in climate science for studying global/regional
16 rainfall characteristics (Masunaga et al., 2020; Satgé et al., 2020), in climate change
17 detection and attribution studies (Paik et al., 2020), event attribution studies (e.g. Wiel et
18 al., 2017), and they are commonly used for climate model evaluation. The satellite rainfall
19 datasets, that have undergone gauge-based correction, can represent rainfall climatology
20 and be used for robust estimation of trends in extreme rainfall (Alexander et al., 2020). An
21 ensemble of these corrected satellite products is useful for studying extremes, especially
22 annual maximum rainfall, and thus can be applicable to data sparse regions (Bador et al.,
23 2020; Nguyen et al., 2020). Another popular choice is to use reanalysis rainfall datasets as
24 they provide a dynamically consistent record of rainfall at finer temporal scale across the
25 Globe.. Reanalyses assimilate irregular observations into a forecast model to simulate
26 temporally continuous estimates of several atmospheric variables over spatially
27 homogenous grids (Sun et al., 2018). Products from these above three categories can also be
28 ‘merged’ together and used for studying rainfall characteristics under various climate
29 regimes (Beck et al., 2017). Merged products, produced by combining rainfall records from
30 gauge-based, satellite and reanalysis datasets, provide reliable estimates of rainfall
31 extremes at Global and regional scale (Rajulapati et al., 2020; Chen et al., 2020). Therefore,
32 it is increasingly important to evaluate these datasets for studying extreme rainfall

1 behavior at regional scale (Fischer and Knutti et al., 2015) and here we perform such an
2 analysis for India.

3 At present various gridded rainfall datasets are available including those from the
4 Frequent Rainfall Observations on Grids (FROGS) database (Roca et al., 2019). Global
5 gauge-based gridded datasets lack good station coverage in the South Asian domain and in
6 India (Nguyen et al., 2020). Regional gridded datasets such as the Asian Precipitation
7 Highly Resolved Observational Data Integration Towards Evaluation of Water Resources
8 (APHRODITE) provide good estimates of large scale monsoon rainfall when compared to
9 the IMD regional gridded dataset (Rajeevan and Bhate, 2009). However, the APHRODITE
10 lacks good station coverage (Nguyen et al., 2020) in East Coast, North central plain, North
11 West and North-Eastern parts of India (Rana et al., 2015). A comparison of the
12 APHRODITE with IMD gridded data found poor correlation for these areas (Rajeevan and
13 Bhate, 2009). They also noted that rainfall in the Western Ghats and NE parts of India is
14 underestimated (bias >3mm/day) in APHRODITE and the maximum rainfall is also
15 underrepresented by this dataset. The high resolution IMD gridded data, which is an
16 improvement over previous generation IMD grid-datasets is found to better resolve the
17 rainfall climatology in India especially in the Western Ghats (Fig. 1) and the core monsoon
18 region (For more details on development of this data see Pai et al., 2014). Pai et al., (2014)
19 compared APHRODITE along with other coarser resolution IMD datasets and observed
20 that rainfall features including heavy rainfall areas in the mountainous belts of the West
21 coast and NE India, and low rainfall in the lee ward side of the Western Ghats are more
22 realistic and better presented in the IMD dataset due to its higher spatial resolution and to
23 the higher density of stations compared to other regional datasets. Therefore, for analyzing
24 regional rainfall patterns, extremes and comparing other gridded rainfall products this
25 high resolution IMD (Pai et al., 2014) data has become a popular choice to climatologist.

26 Recent studies suggest that extreme rainfall over some areas of India has increased in the
27 last few decades. Roxy et al., (2017) reported that central India has experienced a threefold
28 rise in extreme rainfall events due to increasing moisture variability from the Arabian Sea.
29 Significant increase in extreme rainfall events over the southern parts of India and
30 decrease in the northern parts since 1970s is noted by Bisht et al., (2018), which is
31 subsequently corroborated by Dash and Maity (2019). Mukherjee et al., (2018) attributed

1 these changes to anthropogenic forcing using a suite of CMIP5 experiments with and
2 without human GHG emissions. In these circumstances, it is essential to understand how
3 gridded rainfall datasets from various sources can capture these recent observable trends in
4 extreme rainfall events, which have become more prominent in the last few decades over
5 some areas of India.

6 Previous gridded data inter-comparison studies mainly focused on the mean state of climate
7 while assessing their reliability for climatological application (Rana et al., 2015; Fallah et
8 al., 2019). Gridded datasets have also been compared for drought characterization (Zhan et
9 al., 2016; Golian et al., 2019; Chen et al., 2019) and hydrological modelling (Bhattacharyya
10 and Sanyal 2019; Kolluru et al., 2020) in different parts of the world. Since extreme rainfall
11 events are particularly important in triggering natural hazards and determining rate of
12 erosion, it is imperative to focus on extreme rainfall while comparing gridded datasets from
13 different sources. Some recent analyses have assessed the reliability of these gridded
14 datasets in capturing extreme precipitation characteristics on global (Alexander et al.,
15 2020; Bador et al., 2020) and regional scale (Kim et al., 2019; Timmermans et al., 2019;
16 Cavalcante et al., 2020). However, these studies are limited to the analysis of a small
17 subset of available gridded datasets or given lesser emphasis to extreme rainfall
18 characteristics especially in data-sparse country like India (Bharti et al. 2016; Mondal et
19 al., 2018; Singh et al., 2019; Prakash, 2019; Gupta et al., 2019).

20 Nguyen et al., (2020) showed that the magnitude of annual maximum daily rainfall in
21 different sub-regions of monsoon Asia exhibits substantial differences especially in regions
22 that are poorly sampled (e.g. India). . Their results revealed that gauge-based and satellite
23 datasets with correction have stronger similarity than un-corrected products especially in
24 regions with higher station densities (e.g. Japan) in line with other studies (Alexander et
25 al., 2020; Bador et al., 2020). While in data-sparse regions such as India, higher
26 inconsistencies are noted among the datasets and the differences are large for higher
27 extremes. However, Nguyen et al., (2020) only assessed the inter-product differences
28 focusing on annual one-day maximum rainfall. On the other hand, the analysis of
29 magnitude, frequency, and duration of rainfall extremes is limited in India.. Therefore,
30 there are still many gaps in our understanding of the behavior and representation of
31 extreme rainfall in different gridded datasets in India in comparison with high-resolution

1 regional gauge based datasets, like IMD gridded data. Owing to the variability of Indian
2 summer monsoon rainfall and recurring occurrences of climatic extremes, it is important to
3 evaluate the ability of gridded rainfall datasets in reproducing extreme rainfall
4 characteristics.

5 Therefore, the objectives of this study are (1) to compare twelve gauge-based, satellite-
6 derived, reanalysis, and merged rainfall datasets for their suitability to study magnitude,
7 frequency, and duration of extreme rainfall events over different regions of India (2) to
8 assess their performance in reproducing the spatial pattern of observed trends in frequency,
9 duration, and magnitude based indices of extreme rainfall and (3) identify the better
10 performing gridded datasets among the selected ones for extreme rainfall studies. In order
11 to compare these rainfall products, a high resolution ($0.25^\circ \times 0.25^\circ$) and purely gauge-based
12 gridded rainfall dataset, obtained from IMD, is used. The main reason for selecting IMD
13 gridded data as the reference dataset is that it is developed from higher number gauge
14 observations in India than other gauge-based datasets (Fig. 1) and it better represents the
15 orographic rainfall than other gauge-based products (Pai et al., 2014; Bharti et al., 2015).

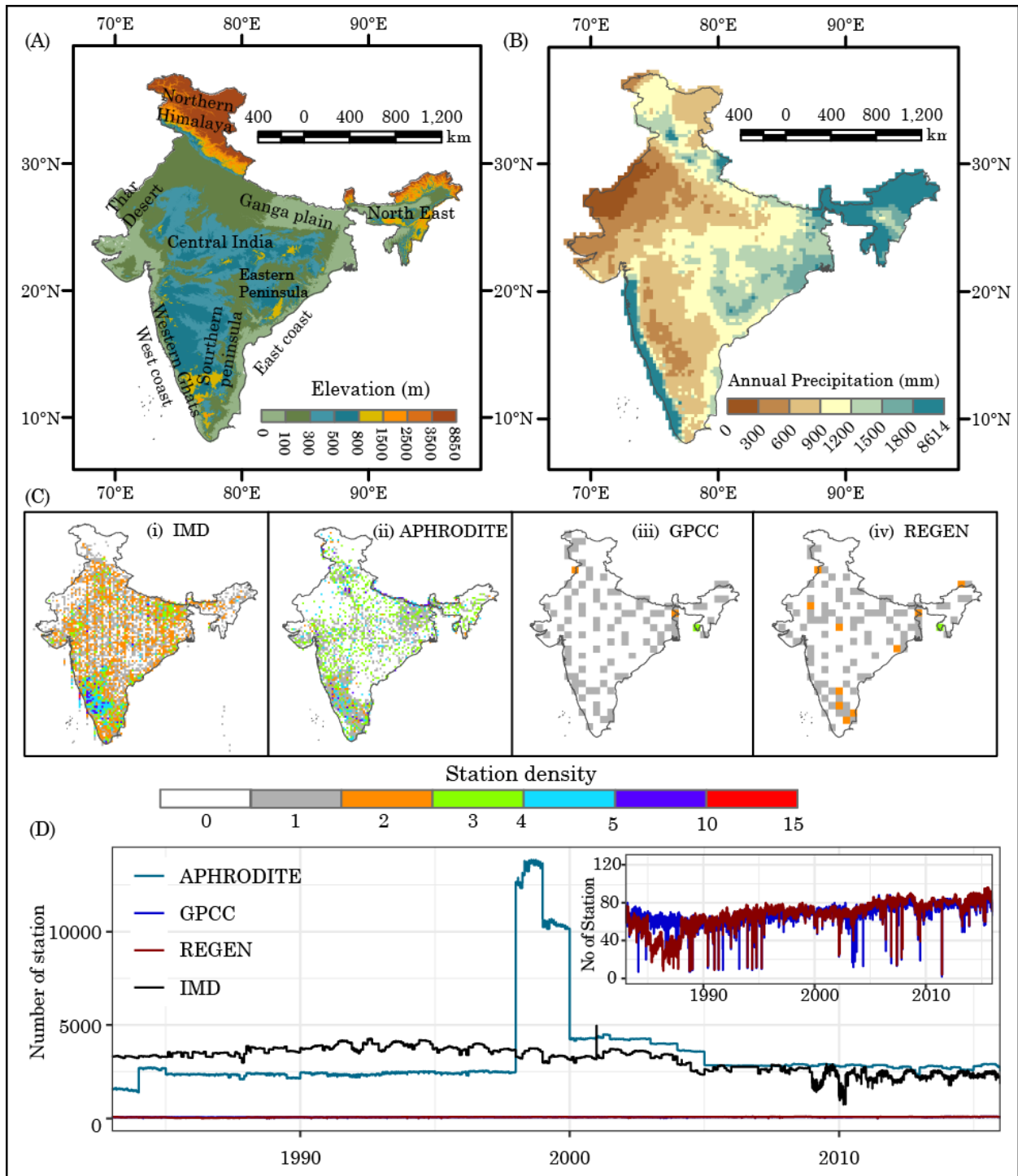
16 **2. Materials and methods**

17 **2.1 Study area**

18 To analyze extreme rainfall events in India, smaller homogenous regions are identified
19 based on physiographic divisions and spatial rainfall patterns (Fig. 1A). These regions are
20 Thar Dessert (TD), Northern-Himalaya (NH), Ganga plain (GP), North-East (NE), Central
21 India (CI), Eastern Peninsula (EP), Southern Peninsula (SP), Western Ghats (WG), West
22 Coast (WC), and East coast (EC). Annual average rainfall over India increases from
23 $<200\text{mm}$ (in TD) to $>6000\text{mm}$ (NE India) following the west to east rainfall gradient.
24 Monthly rainfall in most of these regions reaches its peak during June-September with the
25 arrival of South-West monsoon. An exception to this is observed in parts of southern EC
26 and SP region, where rainfall mostly occurs during post-monsoon (SON) months with the
27 reversal of the monsoon system.

28 **2.2 Datasets**

1 At present different global and regional gridded-rainfall datasets are available at daily
2 temporal scale from various sources, which are categorized as gauge-based, satellite,
3 reanalysis, and merged/blended products. This study make use of twelve of these products
4 having a grid resolution finer than 1 degree with continuous daily records of at least 30
5 years since 1983 (Table 1). Thus, five gauge-based (IMD, APHRODITE, CPC, GPCC, and
6 REGEN); two satellite derived (PERSIANN-CDR and CHIRPS); four reanalysis (ERA5,
7 MERRA2, PGF, and JRA-55); and two blended (WFDEI and MSWEP – described later)
8 rainfall products are considered in this study.



1 Fig. 1 (A) Elevation distribution along with major physiographic regions in India and (B)
 2 the distribution of annual average precipitation in India (derived from the IMD gridded
 3 dataset) during the study period (1983 – 2015). (C) Average station density in IMD (i),
 4 APHRODITE (ii), GPCC (iii), and REGEN (iv) gridded datasets in India at their native
 5 resolution; note that the white areas represent no station while light gray represents very

1 sparse station. (D) Temporal variation in daily gauge information used in APHDROFITE,
2 GPCC, REGEN, and IMD datasets in India during the period of 1983 – 2015; in the inset,
3 temporal variation plotted for GPCC and REGEN since number of stations ranged between
4 0-100.

5 The APHRODITE is a high-resolution continental-scale gauge-based dataset developed
6 using the Spheremap interpolation (Willmott et al., 1985) by combining data shared via
7 Global Telecommunication System (GTS) and other data compiled under the APHRODITE
8 project. Unified Climate Prediction Centre (CPC) dataset combines gauge data from
9 national and international agencies using optimal interpolation algorithm (Chen et al.,
10 2008). The Global Precipitation Climatology Center (GPCC) Full Data Daily V2018 (V2)
11 uses ordinary block kriging method to interpolate in-situ observations shared via Global
12 Telecommunication System (GTS) over the Global land surface. The Rainfall Estimates on
13 a Gridded Network (REGEN) is a newly developed gauge-based dataset that combines
14 station observations from multiple sources i.e. Global Historical Climatology Network –
15 Daily (GHCN-Daily) and GPCC using ordinary block kriging method (Contractor et al.,
16 2020). The REGEN dataset with ‘All Station’ version is used in this study.

17 The Precipitation Estimation from Remotely Sensed Information using Artificial Neural
18 Networks–Climate Data Record (PERSIANN-CDR) is quasi-global satellite data, developed
19 using the Gridsat-B1 satellite data and adjusted using monthly dataset of Global
20 Precipitation Climatology Project (Ashouri et al. 2015). Climate Hazards Group InfraRed
21 Precipitation with Station data (CHIRPS v.2) provides blended satellite-gauge information
22 at quasi-global coverage (Funk et al., 2015). MSWEP v2.0 combines satellite data
23 (CMORPH, GridSat, GSMaP-MVK, SM2RAIN-ASCA and TMPA 3B42RT) and the ERA-
24 Interim and JRA-55 reanalyses as well as gauge based products (GPCC, CPC) (Beck et al.,
25 2017). The WATCH Forcing Data-ERA-Interim (WFDEI) combines ERA-interim reanalysis
26 with gauge based datasets using sequential elevation correction (Weedon et al., 2014). The
27 dataset better represent annual daily maximum rainfall over the globe than other datasets
28 (PERSIANN-CDR, MSWEP, ERA-Interim, and NCEP2) when compared to GPCC (Chen et
29 al., 2020) and also outperform other reanalysis in simulating river discharge (Essou et al.,
30 2016).

31 Table 1 Description of gridded rainfall dataset used in this study.

Dataset	Period	Resolution	Data source	References
IMD	1901-Present	$0.25^\circ \times 0.25^\circ$	Gauge-based	Pai et al. (2014)
APHRODITE	1951 – 2015	$0.25^\circ \times 0.25^\circ$	Gauge-based	Yatagai et al. (2012)
CPC	1979 - Present	$0.5^\circ \times 0.5^\circ$	Gauge-based	Xie et al. (2007)
GPCC	1982 - 2016	$1^\circ \times 1^\circ$	Gauge-based	Schamm et al. (2014)
REGEN	1950 - 2016	$1^\circ \times 1^\circ$	Gauge-based	Contractor et al., 2020
CHIRPS	1981 - Present	$0.25^\circ \times 0.25^\circ$	Satellite	Funk et al. (2015)
PERSIANN-CDR	1983 - Present	$0.25^\circ \times 0.25^\circ$	Satellite	Ashouri et al. (2015)
PGF	1948 - 2016	$0.25^\circ \times 0.25^\circ$	Reanalysis	Sheffield et al. (2006)
ERA-5	1979–present	$0.25^\circ \times 0.25^\circ$	Reanalysis	Hersbach et al., (2020)
MERRA-2	1980 - Present	$0.5^\circ \times 0.67^\circ$	Reanalysis	Gelaro et al. (2017)
JRA-55	1958-Present	$0.5625^\circ \times 0.5625^\circ$	Reanalysis	Kobayashi et al. (2015)
MSWEP	1979 - 2016	$0.1^\circ \times 0.1^\circ$	Merged	Beck et al., 2019
WFDEI	1979 - 2016	$0.5^\circ \times 0.5^\circ$	Merged	Weedon et al., (2014)

1

2 The Princeton Global Forcing (PGF) daily dataset is produced by using global observation-
3 based datasets with the NCEP/NCAR reanalysis at 0.25° resolution (Sheffield et. al, 2006)
4 ERA5 is the fifth generation reanalysis from the European Centre for Medium-Range
5 Weather Forecast (ECMWF) with several improvements in model parameterization and
6 higher spatial and temporal resolution than ERA-Interim (Hersbach et al., 2020). The
7 Modern-Era Retrospective Analysis for Research and Applications, version 2 (MERRA- 2),
8 atmospheric reanalysis is the newest reanalysis product by NASA’s Global Modeling and
9 Assimilation Office (GMAO) replacing the previous generation MERRA product. It uses the
10 new version of the GEOS-5 atmospheric model and includes more observational data,
11 recent satellite observations, and an improved assimilation model (Molod et al. 2015). The
12 Japanese 55-year Reanalysis (JRA-55) is the second reanalysis product from the Japan
13 Meteorological Agency (JMA) which is an improved version of the previous JRA-25 and uses

1 a 4D-VAR approach for data assimilation and variational bias correction technique
2 (Kobayashi et al. 2015).

3 The gridded rainfall data, obtained from the IMD is used as the reference dataset as it has
4 been produced using the largest number of observational stations (N = 6955) in India,
5 compared to other gauge-based gridded data that is available to date. We acknowledge that
6 even fine-resolution gridded products based on large number of gauge data exhibit biases
7 and are known to underestimate rainfall extremes (King et al. 2013; Gervais et al. 2014).
8 The IMD dataset has a spatial resolution of 0.25° with daily rainfall records from 1901 –
9 2015 and it has been adjusted for orographic and other controlling factors of rainfall
10 distribution over India (Pai et al., 2014; Pai et al., 2015; Bharti et al., 2015). Over Indian
11 subcontinent, global datasets (i.e. GPCC, CPC, and REGEN) have poor station coverage. As
12 noted in Nguyen et al. (2020), in the 2000s the station number in APHRODITE in India
13 decreases although it is relatively higher than the IMD dataset. Moreover, the IMD dataset
14 has higher number of station than APHRODITE for pre-1998 period and has better spatial
15 coverage than other datasets. Regional rainfall distribution is also better represented by
16 this high-resolution IMD gridded dataset (see Pai et al., 2014; Pai et al. 2015 for more
17 details) and also used in detecting cloud-burst events over NH (Jena et al., 2020).
18 Therefore, the results from the selected gridded datasets are compared with the IMD
19 dataset.

20 **2.3 Methods**

21 Study of extreme rainfall is carried out in two ways, either by fitting parametric extreme
22 value distribution to assess rare events or by using non-parametric methods of calculating
23 indices for extreme rainfall events, solely based on empirical data analysis. Here we used
24 the non-parametric approach by calculating eleven extreme rainfall indices (Table 2) to
25 encompass a wider range of the extreme rainfall climatology in India, based on absolute
26 and percentile based rainfall thresholds, to evaluate gridded rainfall datasets. Out of these
27 eleven indices, eight indices are selected from ETCCDI (for more details see
28 http://etccdi.pacificclimate.org/indices_def.shtml) and have been widely used for detection,
29 attribution and climate change projection studies around the world (Cavalcante et al., 2020;
30 Dash and Maity, 2019; Kim et al., 2020; Schoof and Robeson, 2016; Srivastava et al., 2020).
31 The other three indices are selected from the IMD rainfall intensity classes (IMD, 2015).

1 We considered only the last three IMD rainfall intensity classes with rounding of the
 2 intensity values namely: heavy rainfall (HR) (65 to 115 mm), very heavy rainfall (VHR)
 3 (115 to 205 mm) and extremely heavy rainfall (EHR) (≥ 205 mm).

4 Extreme indices, characterizing different magnitude (RX1day, RX5day, R95p and R99p),
 5 frequency (R10mm, R20mm, HR, VHR, EHR) and duration (CDD, CWD) of annual extreme
 6 rainfall in India are calculated from daily wet day rainfall, over each grid-cell, resulting in
 7 one value per year for each gridded rainfall product. In this study, a wet day is defined as a
 8 day with rainfall ≥ 1 mm (Chaudhary et al., 2017).

9 The spatial resolution of selected gridded rainfall datasets varies widely from 0.25° to 1°
 10 (Table 1) thus hindering direct comparison with the reference (IMD) dataset. Re-gridding
 11 from higher to lower resolution affects localized extreme rainfall values as higher extreme
 12 values get reduced through the process of averaging. ‘The order of operation’ in calculating
 13 extreme rainfall indices and interpolating to the target grid for comparison has substantial
 14 effects on the representation extreme rainfall values (Herold et al., 2017). Previous studies
 15 shown that the effects of first re-gridding to coarser grid and then calculating extreme
 16 indices can be eliminated by changing the order of operation (Avila et al., 2015; Herold et
 17 al., 2017). Therefore, in this study, the extreme rainfall indices are first calculated at the
 18 native resolution of the datasets and then interpolated to a common 1° grid for a fair
 19 comparison among the datasets.

20 Differences between IMD and other gridded datasets are expressed in terms of percentage
 21 BIAS (PBIAS) and calculated following Eq.1.

$$22 \quad PBIAS = \frac{\sum_{i=1}^n (R_{si} - R_{oi})}{\sum_{i=1}^n (R_{oi})} \times 100 \quad \text{Eq. 1}$$

23 Where R_{oi} is the i^{th} observation from IMD gridded data, R_{si} is the corresponding i^{th}
 24 estimated rainfall from other gridded datasets.

25 Table 2 Extreme rainfall indices recommended by ETCCDI and IMD (highlighted in bold)
 26 considered in this study.

Category	Index	Index Name	Description	Unit
	RX1day	Maximum 1-day rainfall	Annual 1-day maximum rainfall	mm

Magnitude	RX5day	Maximum 5-day rainfall	Annual 5-day maximum rainfall	mm
	R95p	Very wet days	Annual rainfall above long-term 95 th percentile	mm
	R99p	Extremely wet days	Annual rainfall above long-term 99 th percentile	mm
Frequency	R10mm	Number of 10mm or more rainfall days	Annual count of days when daily rainfall $\geq 10\text{mm}$	days
	R20mm	Number of 20mm or more rainfall days	Annual count of days when daily rainfall $\geq 20\text{mm}$	days
	R65mm	Heavy Rain (HR)	Number of days with daily rainfall (R) $65\text{ mm} \leq R < 115\text{ mm}$	days
	R115mm	Very Heavy Rain(VHR)	Number of days with daily rainfall (R) $115\text{ mm} \leq R < 205\text{ mm}$	days
	R205mm	Extremely Heavy Rain (EHR)	Number of days with daily rainfall $\geq 205\text{ mm}$	days
Duration	CDD	Maximum length of consecutive dry days	Maximum number of consecutive days with daily rainfall $< 1\text{mm}$	days
	CWD	Maximum length of consecutive wet days	Maximum number of consecutive days with daily rainfall $\geq 1\text{mm}$	days

1

2 In addition, the probability density functions (PDFs) of average extreme rainfall from
3 twelve other datasets are compared to the PDF from IMD to explore how well these
4 datasets resemble the average spatial distribution of different rainfall indices in India. For
5 this, long-term average values of extreme rainfall indices from all the grid cells in India are
6 considered. Here, the PDFs are estimated using a nonparametric smoothing technique, the
7 Kernel Density Estimator (KDEs) to reduce the sampling error associated with the choice of
8 distribution functions. A Gaussian kernel is used to develop the KDE (Teegavarapu et al.,
9 2013). The temporal variations in average extreme rainfall values in India in different
10 datasets are compared using line graphs.

11 The direction (increasing/decreasing) and magnitude of the trend in extreme rainfall indices
12 over each grid-cell are calculated using the non-parametric Mann-Kendall test (Mann,
13 1945; Kendall, 1948) and Sen's slope estimator (Sen, 1968) for the study period of 1983 -
14 2015. The trend analysis is performed to assess whether the gridded datasets can reproduce

1 the observed trends in extreme rainfall in India or not. The calculation of PBIAS, PDFs and
2 trends are done after re-gridding the extreme indices to a common 1° grid.

3 **3. Results**

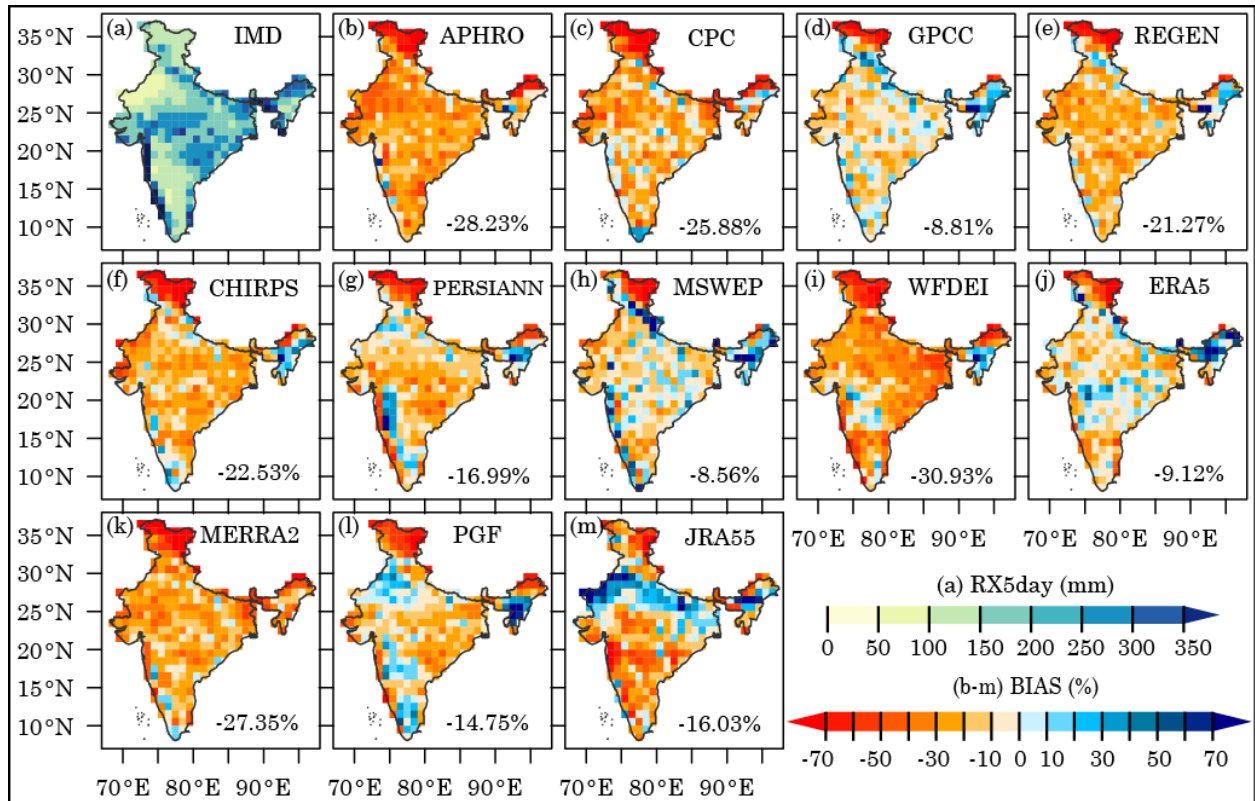
4 In order to compare the datasets, we calculated eleven rainfall indices (Table 2). However,
5 considering the limited length of the manuscript, two magnitude-based (RX5day and R95p),
6 three frequency-based (R20mm, HR, VHR) and two duration-based indices (CDD and CWD)
7 are presented in the manuscript, where other indices are presented in the supplementary
8 information (RX1day, R99p, R10mm and EHR).

9 **3.1 Magnitude of extreme rainfall**

10 In the orographic rainfall zones of WG, NH, NE (Meghalaya plateau) and parts of CI, EP,
11 and GP regions average RX5day rainfall is high (>250 mm). In the dry parts of SP and TD,
12 it is below 150 mm whereas in remaining areas of India it is between 150 mm and 250 mm.
13 Compared to the IMD data, other gridded datasets mostly underestimate (dry bias) RX5day
14 rainfall in India (Fig. 2). Relatively greater underestimation (above 60%) is noted in the
15 orographic belts of NH in all datasets. It tells datasets are unable to capture the orographic
16 influence on rainfall distribution. It should be noted that the gauge density in this region is
17 very sparse especially in the eastern parts of NH and that may explain the higher bias in
18 representing extreme rainfall, especially in the higher elevation zones. Among the gauge-
19 based products, GPCC has better agreement with IMD with a lower bias (Fig. 2d) and also
20 better represents temporal variability of RX5day rainfall (Fig. 3c) than APHRODITE, CPC,
21 and REGEN. Except MERRA2, most of the datasets show overestimation of RX5day
22 rainfall in parts of NE India. Similar overestimation (bias >30%) is found in the SP region
23 in PERSIANN-CDR, MSWEP, and PGF. The JRA-55 overestimates RX5day rainfall over
24 GP and NW India. Overall, APHRODITE, WFDEI, and MERRA2 show higher amount of
25 dry bias while the GPCC, WFDEI, and ERA5 exhibit relatively lower bias in most parts of
26 India. Similar spatial pattern of dry and wet bias is noted for RX1day rainfall (Fig. S1).
27 However, the amount of dry bias is relatively higher for stronger extreme events (RX1day)
28 and comparatively milder extremes (RX5day) rainfall.

29 Comparison of PDFs (Fig. 3a) suggests that except for GPCC, MSWEP, and ERA5 all other
30 datasets overestimate the area of India with RX5day rainfall below ~200 mm and

1 underestimate the area with rainfall above 200 mm (Fig. 3a). This further indicates that
2 the higher extreme rainfall amounts are underestimated by the gridded datasets whereas
3 the tendency of overestimating relatively lower values of extreme rainfall is common,
4 especially over the mountainous belts and dry parts of India. PGF reanalysis is unable to
5 capture RX5day and R95p above 200 mm (Fig. 3a& 3b) whereas the recent generation ERA-
6 5 reanalysis gives more comparable estimates of extreme rainfall to the IMD dataset.
7 Compared to absolute values of higher rainfall indices i.e. RX5day and RX1day, the spread
8 of PDFs is lower for percentile based indices i.e. R95p and R99p. This may due to the
9 independent structure of rainfall distribution and percentiles among these products rather
10 than higher specific amounts that are relatively hard to capture especially by the satellite
11 and reanalysis products. Temporal variations of RX5day and R95p are better represented
12 by GPCC, MSWEP, and ERA5 among their respective groups. In contrasts, WFDEI and
13 PGF underestimate the temporal variability of RX5day and R95p and also have lower CC
14 among the selection of merged and reanalysis products. Similar differences are noted for
15 RX1day and R99p rainfall (Fig. S2) in India

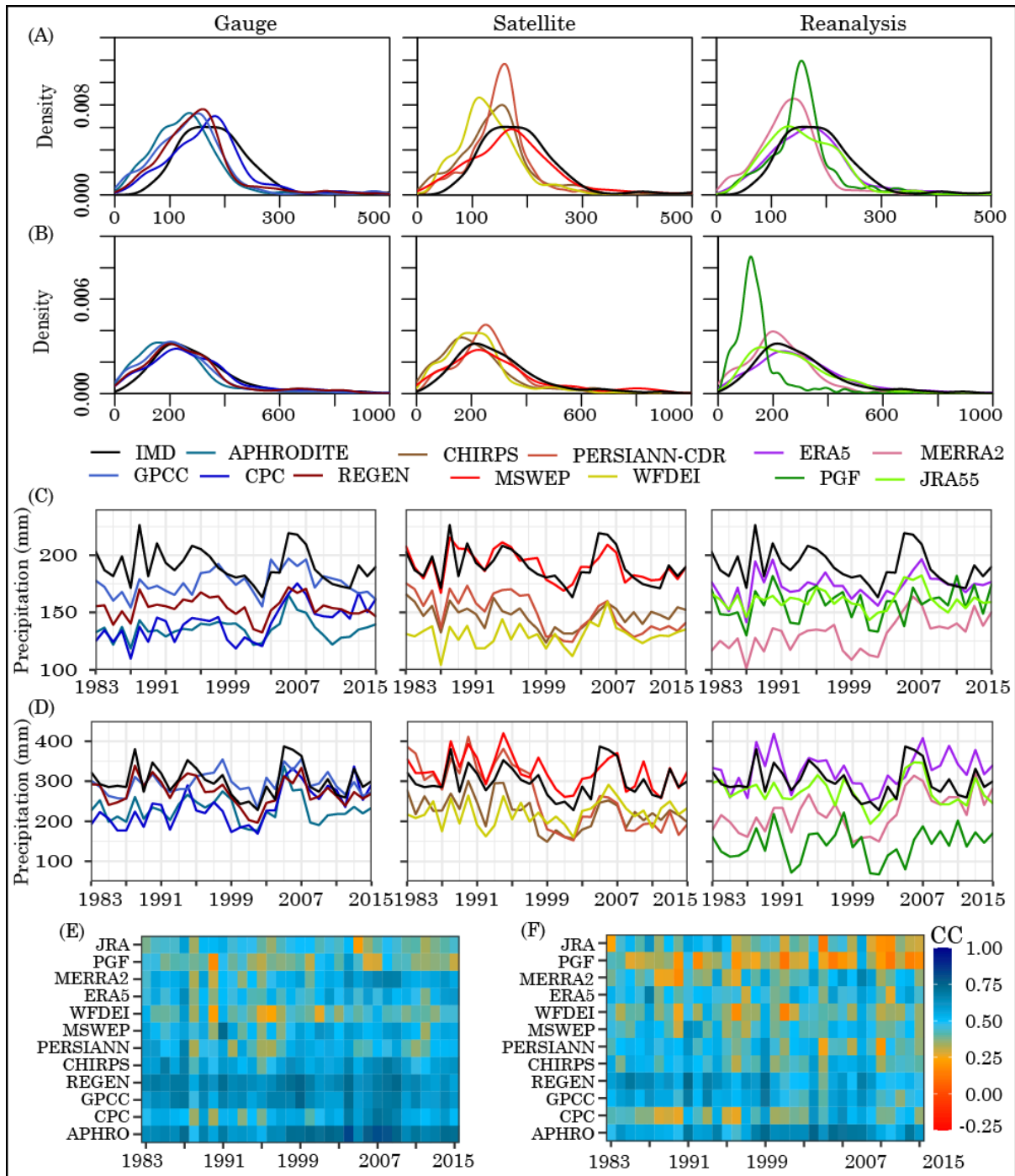


1

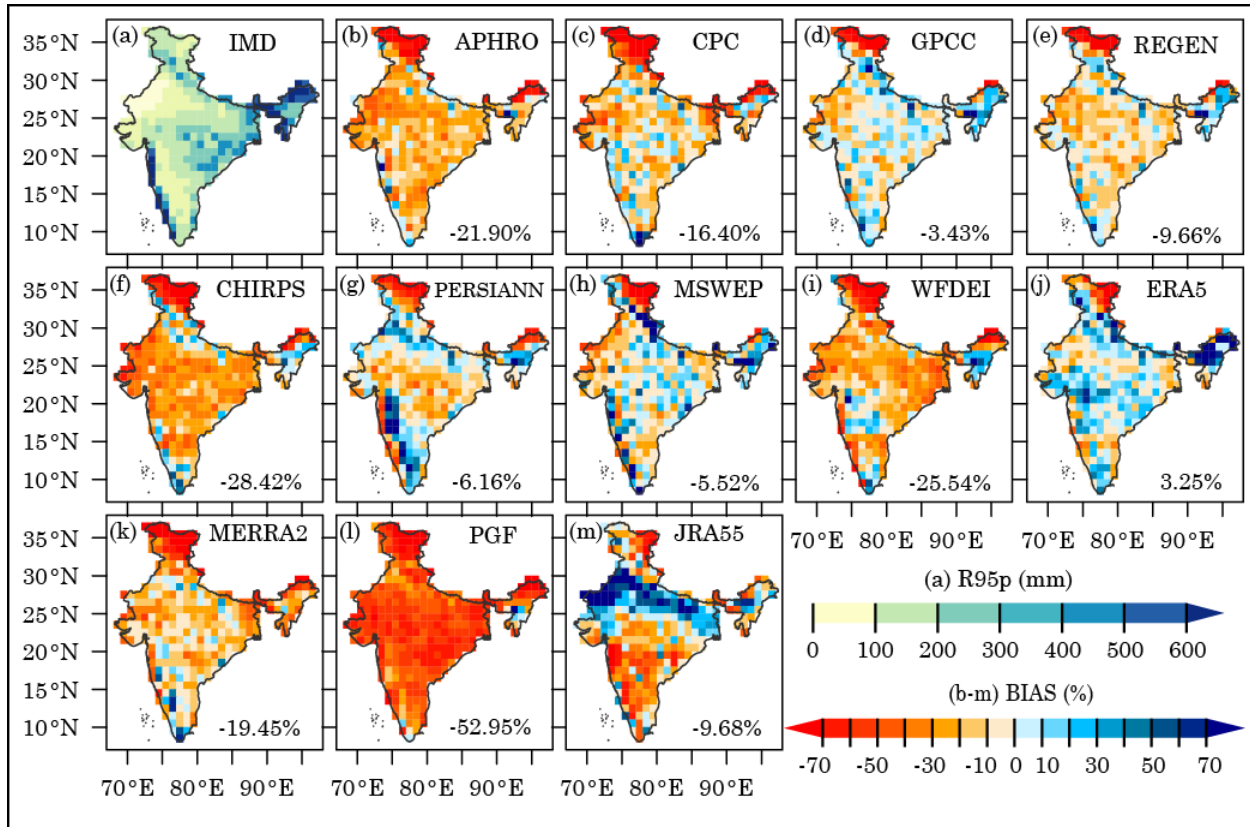
2 Fig. 2. Climatological value of RX5day (over the period of 1983 to 2015) in the IMD dataset
 3 (a) and Percentage BIAS in RX5day from IMD dataset in other rainfall datasets (b-m). The
 4 number inserted in each panel is the median PBIAS in India for respective datasets.

5 Gauge-based datasets have higher spatial correlation with the IMD dataset than other
 6 types of products in representing magnitude RX5day and R95tp in India (Fig. 3e&3f). This
 7 is not surprising given the assimilation of direct rainfall records in these datasets. Among
 8 the gauge-based products, CPC has relatively poor spatial correlation. CHIRPS, MSWEP,
 9 and ERA5 have relatively higher spatial correlation among the satellite, merged and
 10 reanalysis products. PGF reanalysis performed worst among all other products as it greatly
 11 underestimated the spatial and temporal occurrences of magnitude of extreme rainfall in
 12 India. However, the spatial correlation coefficients of these datasets decrease for higher
 13 extreme i.e. RX1day and R99p (Fig. S2).

14



1 Fig. 3 Probability Density Functions represents climatological values RX5day (A) and R95p
 2 (B) in India during 1983 – 2015. Temporal variation of area averaged RX5day (C) and R95p
 3 rainfall (D) in different in gauge-based (left), satellite & merged (middle) and reanalysis
 4 (right) datasets. Spatial correlation coefficients between IMD and other gridded dataset in
 5 representing RX5day (E) and R95p rainfall (F) in India.



1

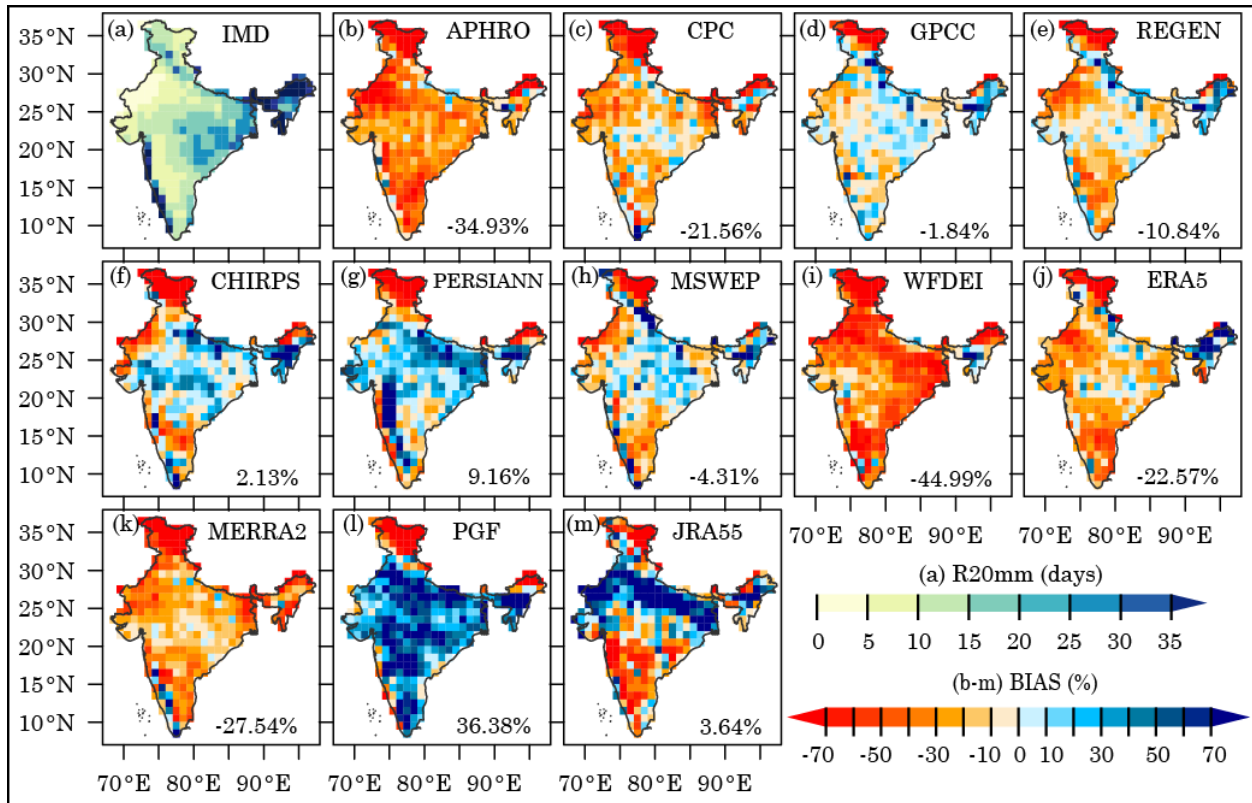
2 Fig. 4. Same as Fig. 2 but for R95p.

3 The spatial pattern of R95p is similar to that for RX5day i.e. areas with higher extreme
 4 rainfall ($R95p > 500$) mm are found over the eastern side of WG and parts of NE India (Fig.
 5 4). In the CI and EP, R95p is between 300-500mm. Similarly, GPCC performs better than
 6 other gauge-based products whereas PERSIANN-CDR, MSWEP, and ERA5 have better
 7 performance than other satellite, merged, and reanalysis products respectively. However,
 8 over the WG region, CHIRPS, PERSIANN-CDR, and MSWEP overestimate R95p (Fig. 4)
 9 and R99p (Fig. S3). This may be due to the overestimation of orographic rainfall over
 10 complex topography by the satellite rainfall datasets which is also noted by Gupta et al.,
 11 2019). Although ERA-5 exhibits lower bias for magnitude based indices than other
 12 reanalysis datasets, it overestimates magnitude of rainfall indices over the NE parts (Fig.
 13 4).

14 **3.1 Frequency of extreme rainfall**

1 Distribution of R20mm closely follows the spatial distribution of annual rainfall in India
2 where relatively higher frequency of R20mm (>30 days/year) can be found in areas where
3 the annual average rainfall is above 1800 mm (Fig. 1b), especially over WG, NE, and in
4 parts of NH (Fig. 5a). In the EP, GP, and parts of NH and CI the R20mm is between 15-30
5 days/year whereas in other areas of India it is below 15 days/year. APHRODITE, CPC,
6 WFDEI, ERA5, and MERRA2 in general show dry bias in India in representing frequency
7 of R20mm. In contrast, CHIRPS, PERSIANN-CDR, PGF, and JRA-55 mostly exhibit wet
8 bias, especially over SP, CI, GP, and NW India. The magnitude of wet bias in these datasets
9 increases for lower rainfall thresholds (R20mm and R10mm) and a mixed pattern of wet
10 and dry bias is noted, compared to the substantial dry bias for higher extreme indices.
11 Lower rainfall i.e. R10mm is more common, especially during the monsoon season. These
12 low rainfall days are generally overestimated in the satellite and reanalysis rainfall
13 datasets. Overestimation of R20mm is highest in PGF over most parts of India, except NH
14 and parts of NE and WG region. This dataset underestimates frequency of R20mm below 20
15 days and overestimates it between 20-40 days (Fig. 6a) which is in contrast to the large dry
16 bias that is found for higher extreme rainfall indices.

17 Similar to magnitude based indices, greater dry bias (>60%) is found in the NH. The PDFs
18 suggest that the gauge-based, satellite, and merged products (except APHRODITE and
19 WFDEI) overestimate R20mm below 10 days but better represent R20mm above 20 days
20 (Fig. 6a). These datasets (gauge-based, satellite and merged) are also better in representing
21 the spatial and temporal variation in R20mm than the reanalysis (Fig. 6b) and can be
22 considered as a useful resource for analyzing lower extremes (e.g. R20mm). In contrast, the
23 APHRODITE, WEDEI, and MERRA2 overestimate R20mm below 10 days and
24 underestimate R20mm above 10days which also explain the underrepresentation of
25 temporal variations by these datasets. Reanalysis datasets have higher inter-product
26 spread than other type of datasets, thus the temporal variations are less consistent among
27 the reanalyses. Similar inconsistencies between reanalyses are also noted globally
28 (Alexander et al., 2020) as well as for Asia and India (Nguyen et al. 2020). . Spatial
29 correlation of R20mm (Fig. 6c) and R10mm (Fig. S5) is higher than the magnitude-based
30 indices. GPCP and REGEN have correlation above 0.8 for most years. This indicates that
31 there is more agreement between IMD and other datasets for lower rainfall thresholds.



1

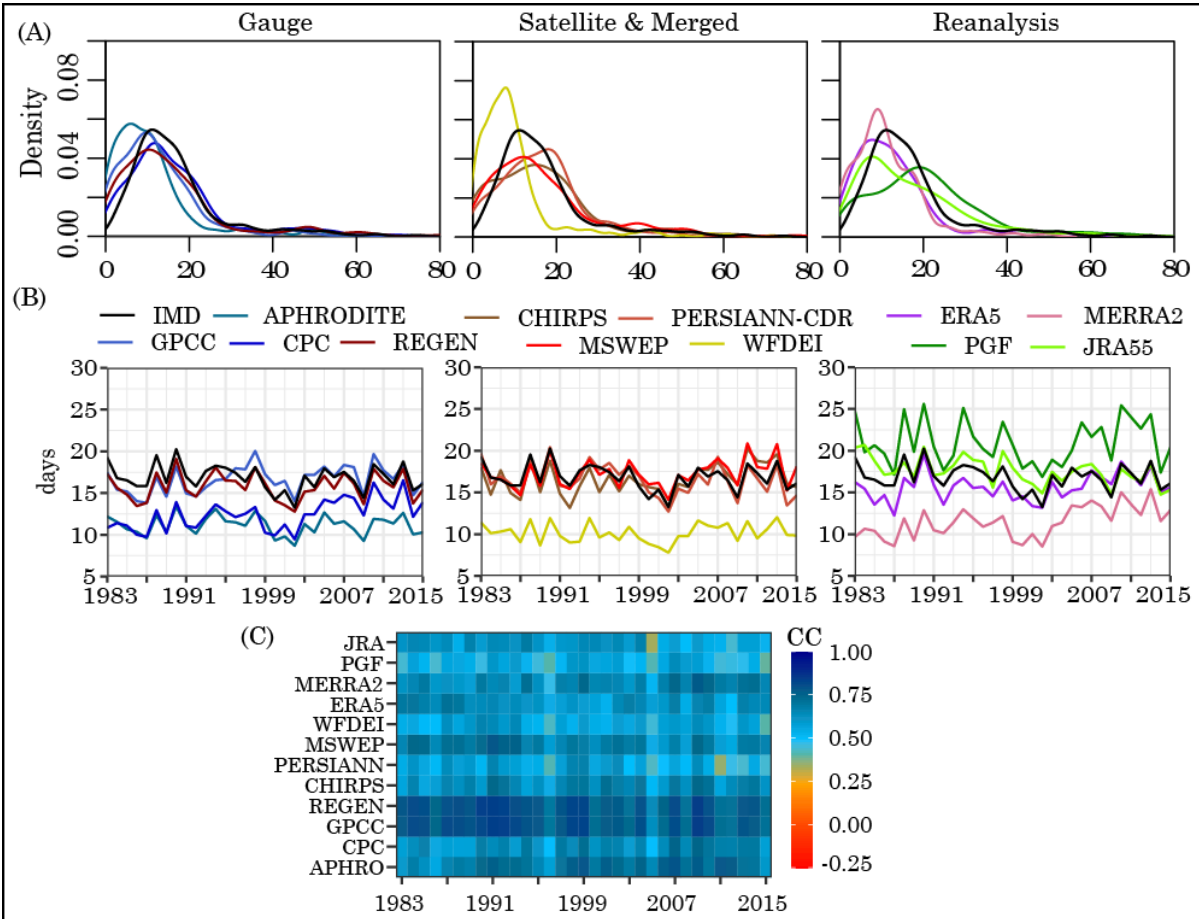
2 Fig. 5. Same as Fig. 2 but for R20mm.

3

4

5

6



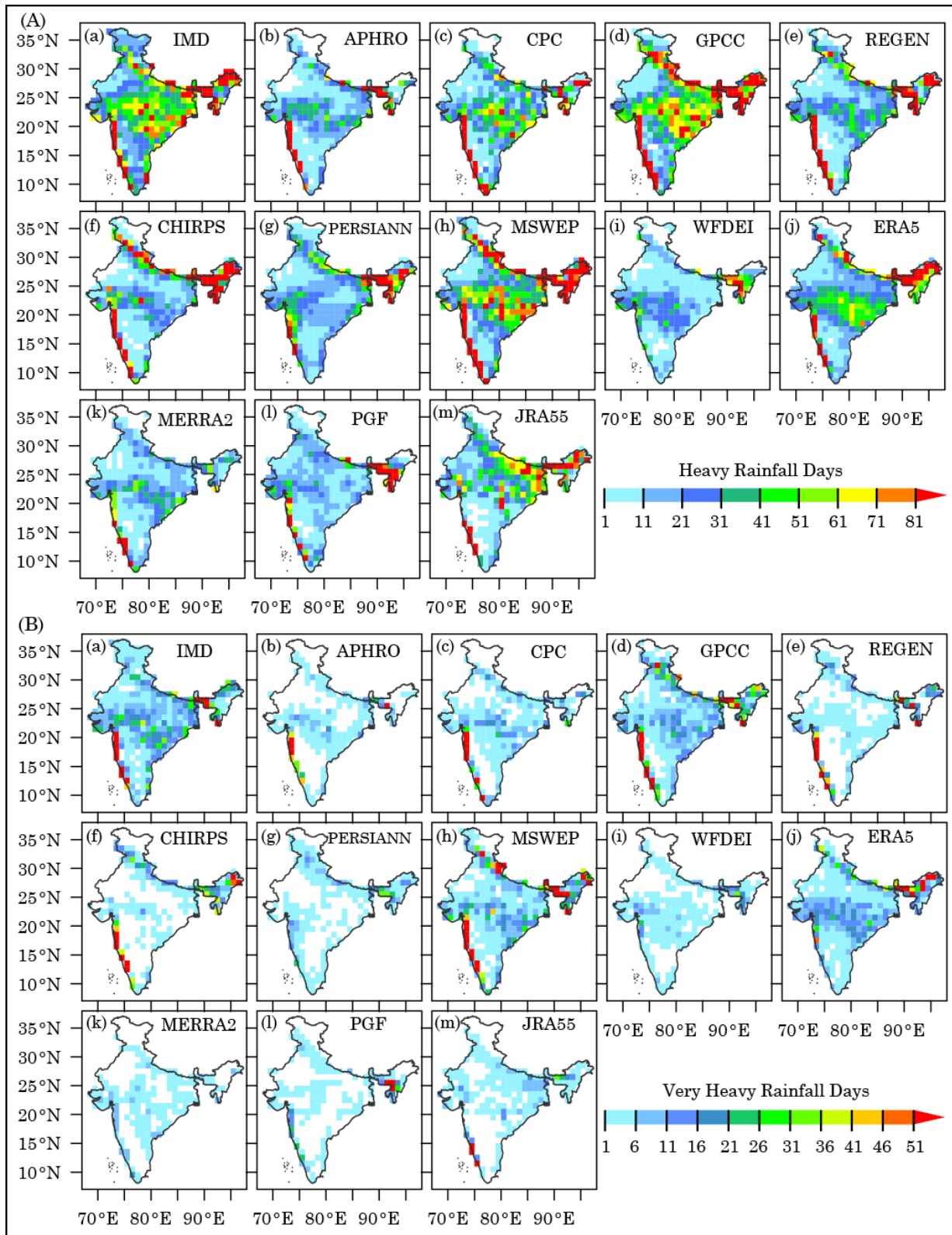
1 Fig. 6. Same as Fig. 3 but for R20mm.

2 **3.3 Heavy, very heavy, and extremely heavy rainfall days**

3 Heavy rainfall (HR) and very heavy rainfall (VHR) events in India are mainly concentrated
 4 in the foothills of the Himalayas, western side of WG, EC, and in parts of the CI and EP
 5 region (Fig. 7). Strong orographic control is found to exist in the occurrences of extreme
 6 rainfall events in India where in parts of WG and NE India, total frequency of HR and VHR
 7 are above 80 and 50 events respectively, during the study period. Moreover, HR and VHR
 8 events are less frequent in dry parts of TD, SP, and NH region, resulting in a lower annual
 9 rainfall amount in these areas. Similar to magnitude-based indices, HR and VHR events
 10 are also greatly underestimated by these datasets. The HR days in the central and eastern
 11 peninsular areas of India are not well captured by the APHRODITE, which may be due to
 12 lower station density in these regions (Fig. 7a). In the satellite-based data, CHIRPS better
 13 represents frequency of HR and VHR than PERSIANN-CDR but overestimates HR
 14 frequency in the Himalayan foothills. MSWEP better estimates HR and VHR and is

1 comparable to gauge-based IMD and GPCC but also overestimates HR frequency over the
2 Himalayan foothills (Fig. 7). The WFDEI is worst among the products analyzed which may
3 stem from the incorporation of ERA-Interim reanalysis in this merged product which is
4 known to underrepresent extreme rainfall in India (Kim et al., 2019).

5 Extremely heavy rainfall (EHR) days (>205mm) are very rare in India but have relatively
6 greater impacts in damaging infrastructure and crops. Similar to HR and VHR, spatial
7 occurrences of EHR only from GPCC, MSWEP, and ERA5 datasets are comparable to IMD
8 (Fig. S6). Only the ERA-5 reanalysis data identified some EHR days over NE, CI, and EP.
9 Overall, the GPCC, MSWEP, and ERA5 give better estimates of higher extreme rainfall,
10 however, with some overestimation in the orographic belts of WG and WH. The
11 improvements in capturing extreme rainfall in ERA-5 over other reanalysis are also noted
12 by (Mahato and Mishra, 2019). In MSWEP, various satellite rainfall datasets are
13 incorporated which are known to overestimate extreme rainfall in the orographic belts in
14 India (Gupta et al., 2019).

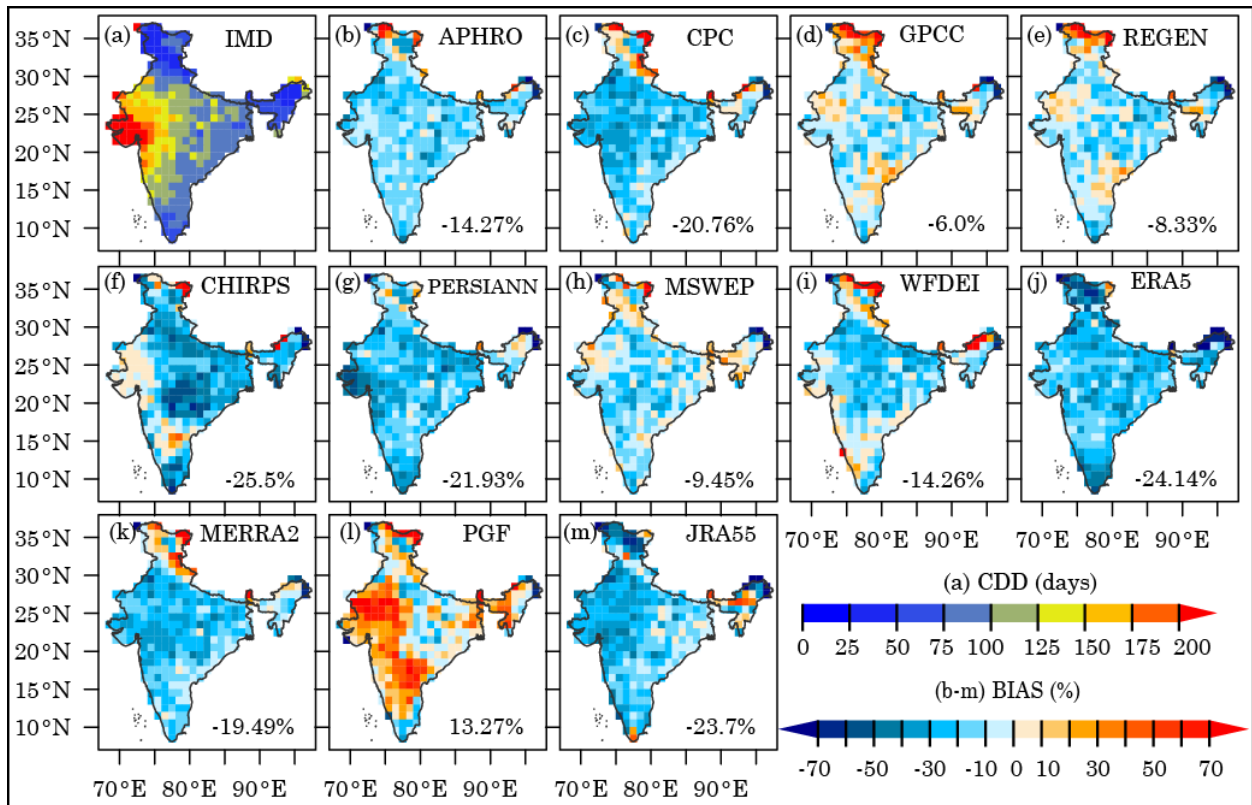


1

2 Fig. 7 Total number of heavy rainfall (HR) and very heavy rainfall (VHR) events in India
 3 during the period of 1983 – 2015.

1 **3.4 Duration based extreme Indices**

2 Dry day duration (CDD) is quite high (>150days) in the arid and semi-arid areas of WI, and
 3 is comparatively short (<50 days) in the NE, southern WG, and NH parts of India (Fig. 8).
 4 Lower CDD in the NH is due to the intermittent rainfall-snowfall occurrences during the
 5 monsoon-winter continuum, influenced by the monsoon and western disturbances
 6 respectively. Except for the PGF, other gridded products underestimate CDD over most
 7 parts of India (Fig. 8). Compared to the IMD dataset, CDD in the PGF is higher (>200 days)
 8 over the WI and SP. GPCCC, REGEN and MSWEP better captured the spatial distribution of
 9 CDD and have median PBIAS less than 10% in India. In general, dry day lengths are
 10 underestimated by the selected datasets in most parts of India.

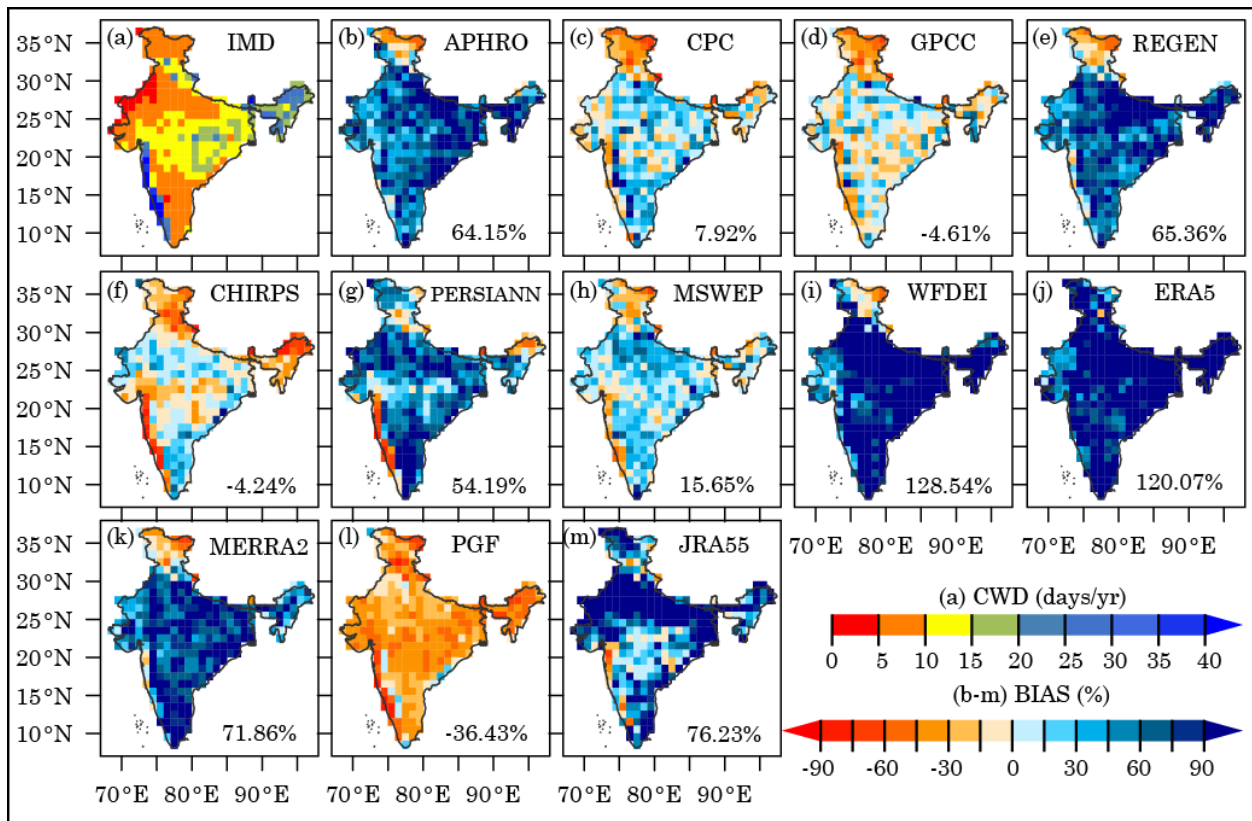


11
 12 Fig. 8. Same as Fig. 2. But For CDD.

13 In contrast to CDD, higher CWD is found over the higher rainfall receiving zones (the WG
 14 and NE parts) and lower CWD values are observed over the dry-regions of western parts of
 15 India, in and around the TD (Fig. 9). The southern WG and NE parts of India are the
 16 wettest because of prolonged rainfall spells during monsoon. In the western parts and

1 southern peninsula, the rainfall is sporadic even during monsoon and this explains the
 2 lower CWD. In the core monsoon region and lower Gangetic plain, wet spell lengths are
 3 moderate and affected by the oscillation of the monsoon trough (Singh et al., 2019). Overall,
 4 CHIRPS and GPCP show strong performance in capturing spatial and temporal variations
 5 (Fig.10) of CWD in India, followed by CPC and MSWEP. Estimated PDFs from these three
 6 datasets (CHIRPS, CPC, and GPCP) are also close to the PDF from IMD. Except for the
 7 PGF, all other reanalyses greatly overestimate CWD in India with median bias above 70%
 8 whereas the PGF underestimates CWD by a similar magnitude.

9



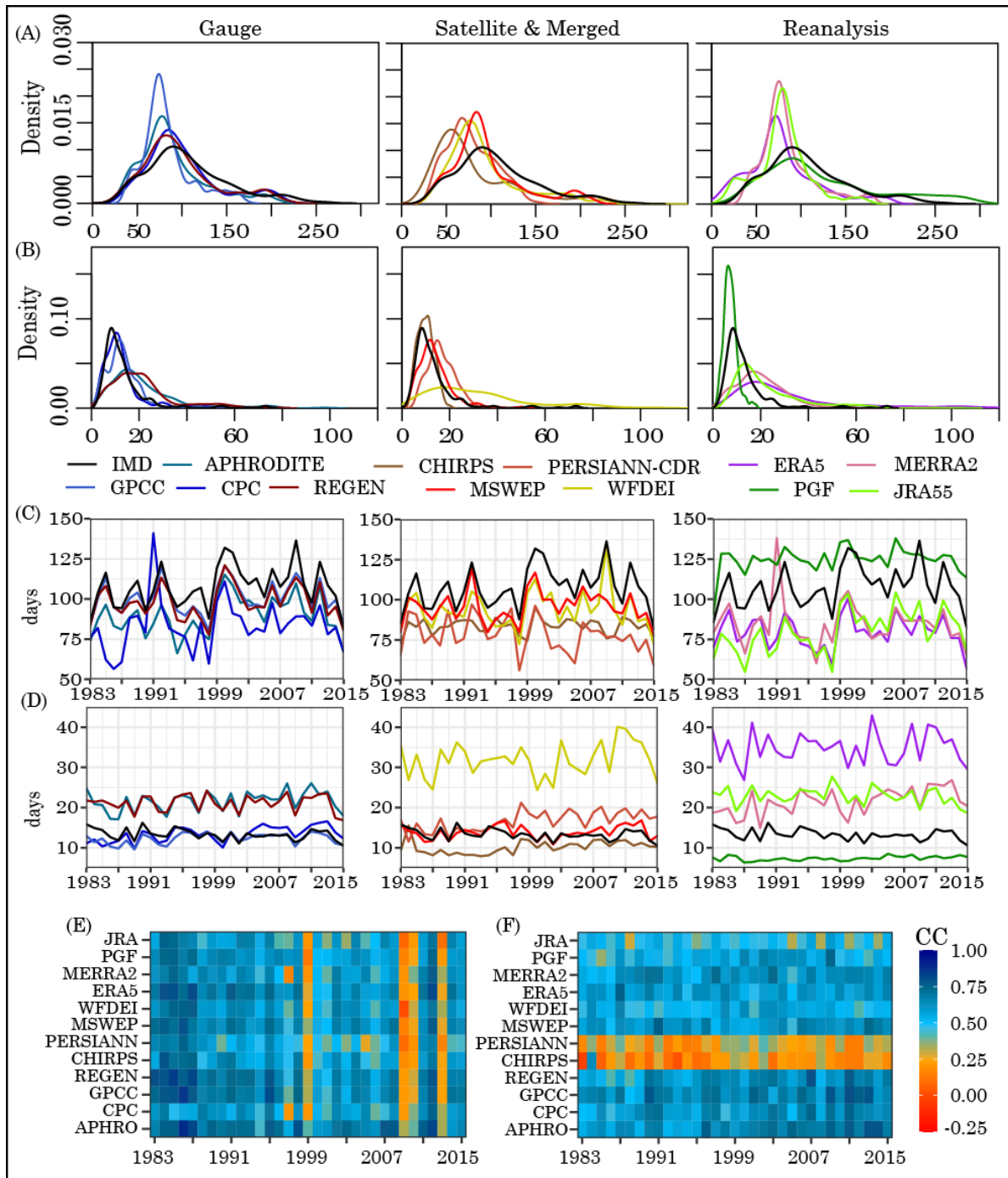
10

11 Fig. 9. Same as Fig. 2. But for CWD.

12 The gauge-based datasets have better agreement with IMD in estimating spatial and
 13 temporal variation in CDD and CWD (Fig. 10). Also, gauge-based and satellite datasets
 14 better estimate CWD than the CDD (except the WFDEI). However, inter-product spread in
 15 reanalysis datasets is relatively higher for both of these indices (Fig. 10). Overestimation of
 16 too many wet days with little rainfall in reanalysis products may be due the numerical

1 forecast model and uncertainties associated with parameterization schemes. This also
2 affects the representation of dry days in these products. Overall, the spatial and temporal
3 variability in (Fig. 10) dry days is better represented by the selected rainfall products than
4 the wet days. Prolonged wet spells in the windward side of Western Ghats and NE during
5 monsoon are due to the mountain-cloud interaction. However, satellite rainfall estimates
6 are based on the relationship of rain rate with cold cloud top temperature measurements.
7 This generates large bias and explains the underestimation of wet day length in the
8 Western Ghats and NE India.

9



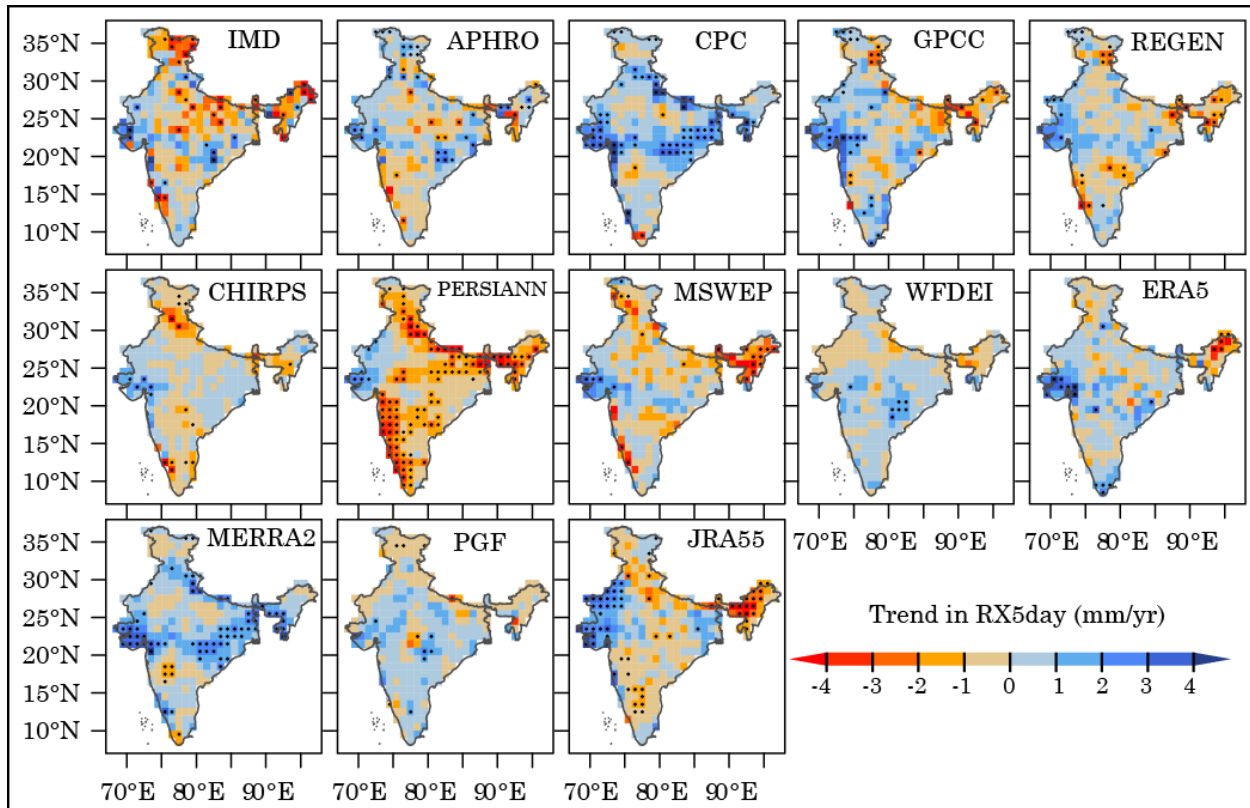
1 Fig. 10 Probability Density Functions represents climatological values CDD (A) and CWD
 2 (B) in India during 1983 – 2015. Temporal variation of area averaged CDD (C) and CWD
 3 rainfall (D) in different in gauge-based (left), satellite & merged (middle) and Reanalysis
 4 (right) datasets. Spatial correlation in representing CDD (E) and CWD rainfall (F) in India
 5 between IMD and other gridded dataset in representing.

6

3.5 Comparison based on trends in extreme rainfall

3.5.1 Trend in extreme rainfall magnitude

RX5day and RX1day rainfall has significantly increased in parts of western India, EP, and south-eastern parts of NH during the study period, whereas it has decreased over large parts of NH, GP, NE, and parts of WG region (Fig. 11 & Fig. S?). Estimated trends in magnitude-based indices in other gridded datasets show largest contrast with respect to the IMD dataset. It should be noted that the significant increasing and decreasing trend points for magnitude based indices are found in isolated places for the IMD dataset, however, these are clustered and found over larger areas in other gridded datasets. The wetting trend over western parts of India and drying trend in NE is present in all datasets (except CPC and MERRA2) with some over and underestimated areas. Trends in RX5day by CPC and MERRA2 are similar and they mostly overestimate increasing (wetting) trend areas over NW, GP, CI, and EP region. Thus, except CPC, other gauge-based datasets are consistent in representing the general pattern of increasing and decreasing trend, especially the wetting trends over EP and western parts of India and drying trend over NE and WG. However, the drying trend over GP and NH is underrepresented by the gauge-based datasets (Fig. 11). The PERSIANN-CDR noticeably shows a drying trend over the orographic belts and other parts of India, however, with the exception in the western parts where the wetting trend is present in almost in all datasets. The MSWEP gives more similar estimates of trend magnitude in RX5day and Rx1day in India and better than other satellite, reanalysis and merged datasets when compared with the IMD dataset. In the reanalysis group, ERA5 and JRA55 also represent the drying and wetting trends in RX5day and Rx1day rainfall over NE and western India respectively. CPC and MERRA-2 exhibited wetting trends whereas the PERSIANN-CDR showed drying trend in most parts of India.



1

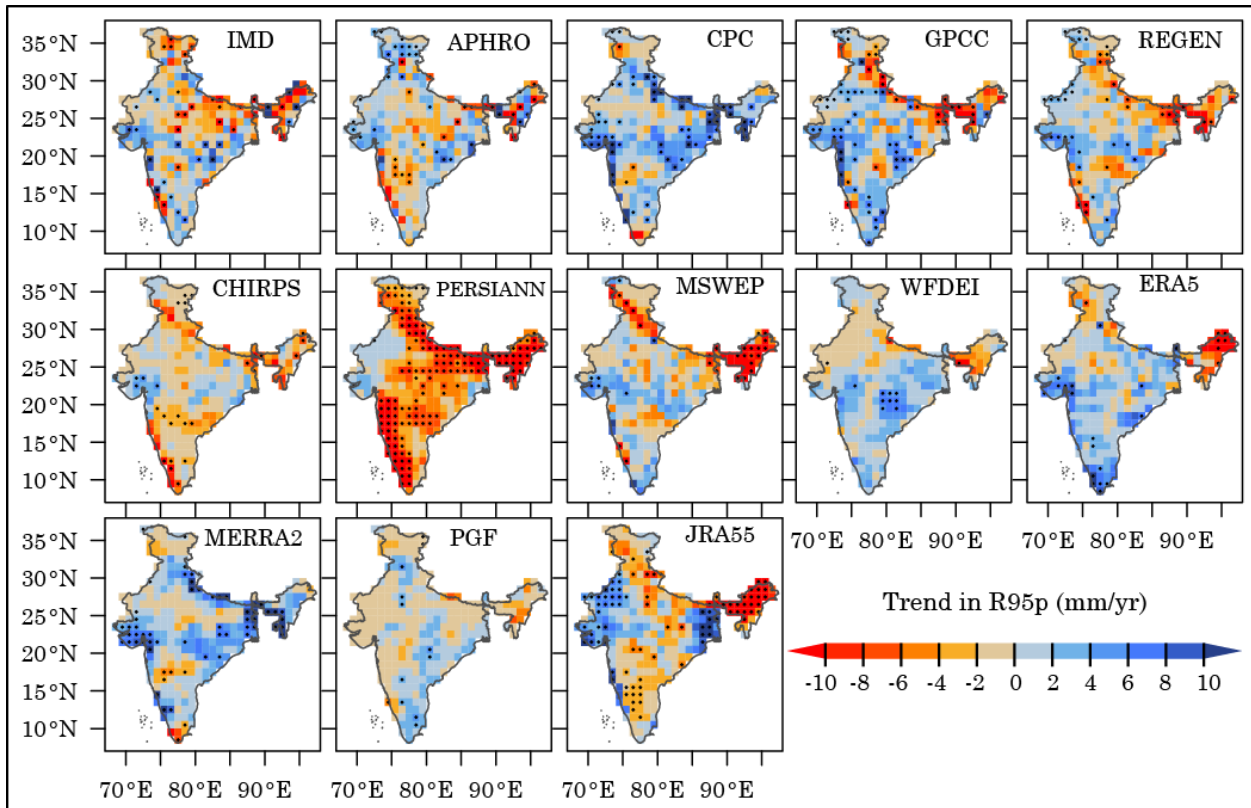
2 Fig. 11. Trend in RX5day rainfall during 1986-2015 in India. Black-dots showing grid-cells
 3 with significant trend at 95% level.

4 Regional patterns of trend direction in R95p are also variable and incoherent in the IMD
 5 datasets but the magnitude of decrease in R95p is relatively higher than RX1day and
 6 RX5day (Fig. 12). This is also true for most datasets, albeit with some showing more
 7 increasing trends (e.g. MERRA2 and CPC) and others more decreasing trends (PERSIANN-
 8 CDR).

9

10

11



1 Fig. 12. Same as Fig. 11 but for R95p.

2 **3.5.2 Trend in extreme rainfall frequency**

3 Significant decreasing trends in R20mm and R10mm (Fig.13 & Fig.) days are observed
 4 mostly in NH, GP, and NE India whereas increasing trends are found over the WG and EP
 5 region of India. This indicates that the drying and wetting trends are consistent with
 6 magnitude based indices resulting in changes in monsoonal rainfall in these regions
 7 (Mahato and Mishra, 2020; Singh et al., 2019). CPC, GPC, and MERRA2 have mostly
 8 showed wetting trend over most part India in contrast to IMD. Besides, the PERSIANN-
 9 CDR which show drying trend R20mm and other magnitude-based indices, has wetting
 10 trends for relative low rainfall days (R10mm).

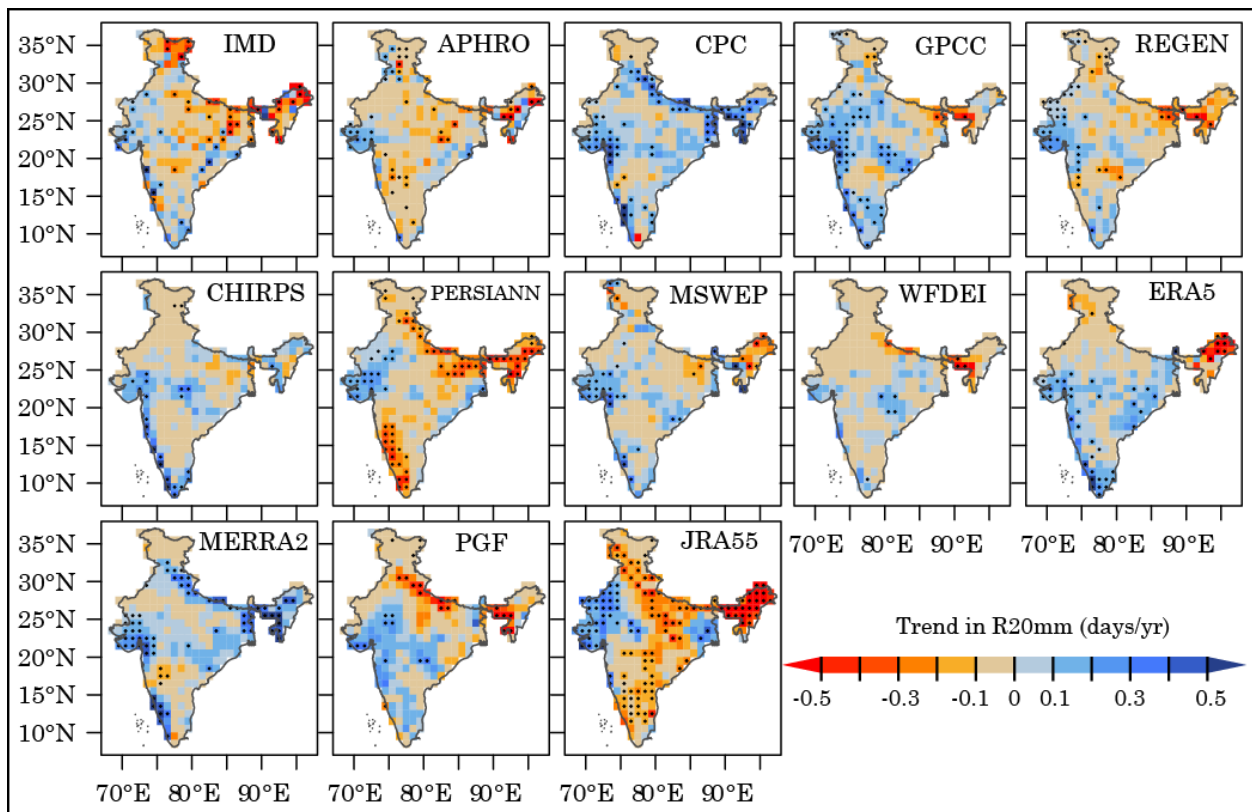
1

2

3 Fig. 13 Same as Fig. 11 but for R20mm.

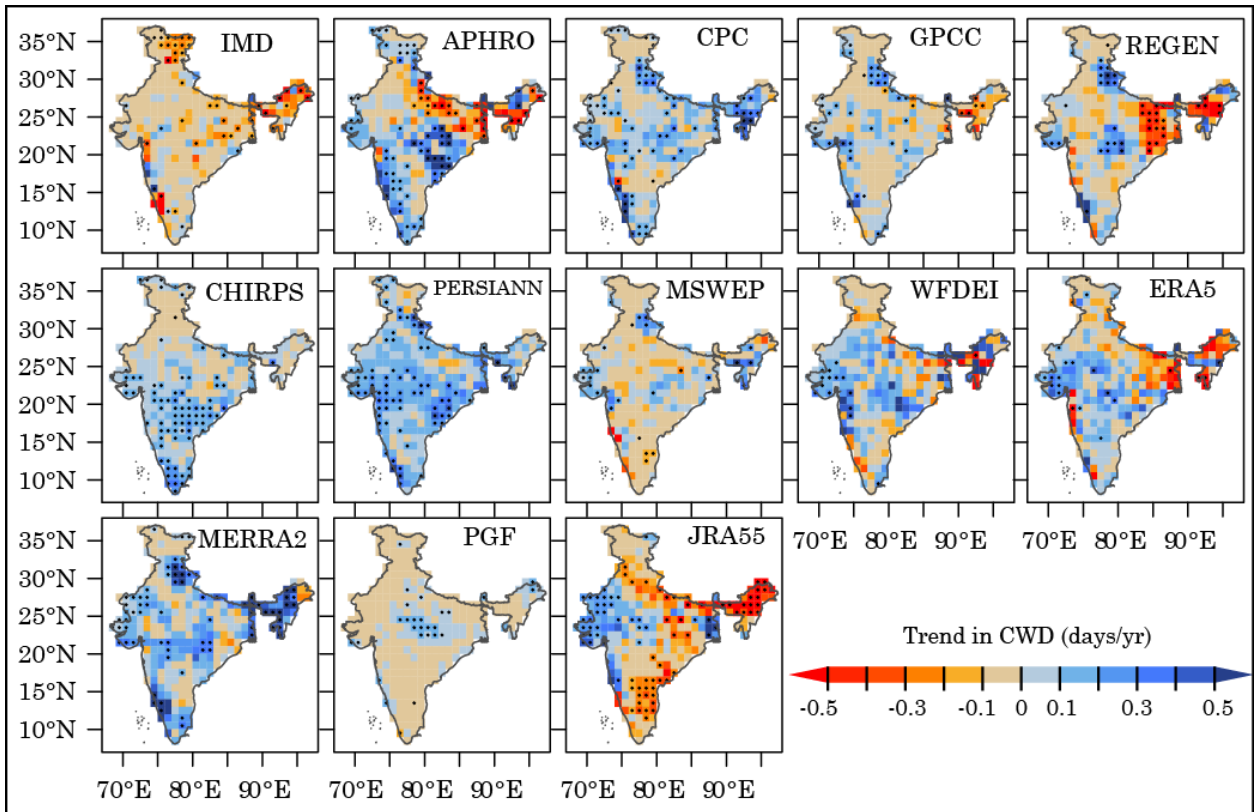
4 **3.5.3 Trend in extreme rainfall duration**

5 For the trends in CWD, large uncertainties are observed across different datasets. Some
 6 datasets (e.g. CPC and MERRA2) has strong wetting trend for all the indices. Most of the
 7 datasets show pattern of increasing trend in CWD over most parts of India in contrast to
 8 the isolated patches of increasing trend of IMD. Compared to other extreme indices, for
 9 CWD higher inconsistencies are noted with the IMD. This may be due to the higher bias
 10 estimating CWD in these datasets. In contrast to that, spatial pattern of trends in CDD are



11 consistent across most of the datasets. However, the JRA-55 has strong increasing trend in
 12 CDD dry days. Overall, the gauge-based datasets (except the CPC) are more consistent with
 13 the IMD in estimating trends in CDD than other products.

14



1 Fig. 14. Same as Fig. 11 but for CWD.

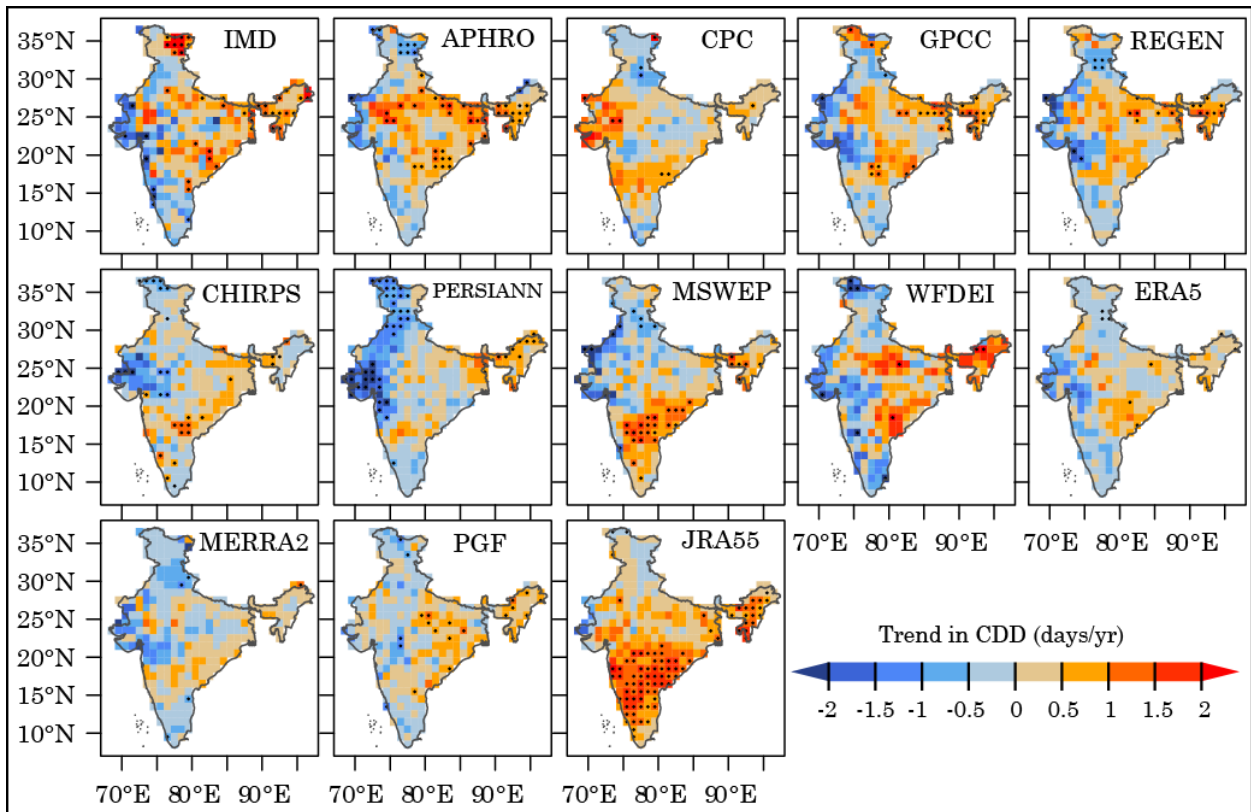
2

3

4

5

6



1 Fig. 15 Same as Fig. 11 but for CDD.

2 **4. Discussion**

3 From the above analysis, it is evident that the relative performance of gridded datasets
 4 varies in India and with the choice of extreme rainfall indices. The dry bias was highest for
 5 higher extreme indices (i.e RX1day and R99p) compared to relatively lower extreme (i.e.
 6 RX5day and R995p. This tail-dependent nature of extreme rainfall bias is a general feature
 7 of the satellite and reanalysis rainfall datasets. Analysis of frequency-based indices also
 8 confirms this, where heavy and very heavy rainfall days highly underrepresented in these
 9 products but R20mm overestimated. This means that the underestimation of extreme
 10 rainfall is mainly compensated by overestimating lower rainfall amounts in these datasets,
 11 which also explain the closer approximation of annual wet day rainfall (not presented in
 12 this study). Underestimation of extreme rainfall in India is noted in all datasets considering
 13 the high-resolution IMD gridded data as reference. However, considering another high-
 14 resolution (APHRODITE) gridded data as reference, Nguyen et al., (2020) found that
 15 extreme rainfall is overestimated over Asian domain as well as in India. Therefore,
 16 highlighting the importance of considering regional dataset such as IMD gridded-data, as it
 17 has higher station density than any other gauge-based dataset in India.

1 the representation of extreme rainfall among the selected gridded datasets varied markedly
2 in India. Among the gauge-based gridded datasets GPCC shows the best agreement with
3 the IMD dataset ahead of REGEN, APHRODITE, and CPC. This is quite surprising given
4 higher station density in APHRODITE in India than GPCC (Fig. 1). APHRODITE has
5 relatively poor coverage over Eastern peninsula and western dry parts of India. GPCC has
6 a higher station density and a homogenous spatial coverage in India (especially in CI and
7 EP region) compared to APHRODITE and CPC (Rana et al., 2015; Schneider et al., 2014).
8 Therefore, GPCC gives close estimate to IMD for most of the extreme indices and also
9 better preserve the spatial variation of rainfall extreme in India. Another source of
10 uncertainty may be due to the differences in interpolation techniques used to construct
11 these datasets. The Spheremap interpolation technique used by GPCC and APHRODITE is
12 found to more robust over complex terrain than the optimal interpolation technique used in
13 CPC (Ahmed et al., 2019; Salman et al., 2019). The gauge-based datasets failed to capture
14 extreme rainfall dynamics over orographic belts, mainly in the eastern parts of the NH.
15 This is mainly due to mere absence of gauge records in these gridded datasets in this region
16 during construction (Pai et al., 2014).

17 Among the satellite rainfall datasets, CHIRPS performs better than PERSIANN-CDR in
18 reproducing extreme rainfall behaviour in India. Similar findings for CHIRPS are also
19 reported by Gupta et al., (2019) in reproducing extreme rainfall in India. Inadequate
20 representation of extreme rainfall over the WG and foothills of NH is a limitation of
21 satellite-derived rainfall as the remotely-sensed precipitation measurements fail to detect
22 orographic rainfall resulting from atmosphere-mountain interactions (Gupta et al., 2019).
23 PERSIANN-CDR uses infrared (IR) measurements of cloud top temperature and its
24 relationship with precipitation rates for providing daily precipitation estimates. To avoid
25 large unrealistic estimates of precipitation, maximum estimates are capped in PERSIANN-
26 CDR system by setting an arbitrary limit, which can explain underestimation in extreme
27 precipitation. Another constraint is that the training of artificial neural network relies
28 solely on the IR measurement and a high-resolution data which is limited over the
29 continental United States only. On the other hand, the CHIRPS precipitation estimates are
30 derived by subsuming data from multiple sources (gauge-based, IR measurements, T3B42,
31 and CFS2). Besides, the CHIRPS uses gauge-based GPCC data for calibration, while the
32 PERSIANN-CDR estimates are calibrated using the GPCP satellite-derived precipitation

1 product. However, these two datasets are inadequate in representing the spatial pattern of
2 extreme rainfall trends in India. The PERSIANN-CDR and CHIRPS are mainly developed
3 to provide temporally homogeneous precipitation records rather than the best
4 instantaneous estimates of precipitation rates. The MSWEP merged product performs
5 reasonably well in representing extreme rainfall events in India and bias is also lower and
6 similar to GPCP. However, over orographic belts it overestimated heavy rainfall events
7 which are similar to GPCP. Chen et al., (2020) noted that WFDEI better capture RX1day
8 over the globe when compared to GPCP. However, this study finds higher bias in India for
9 this dataset. Higher extreme rainfall events as well as the magnitudes of their changes are
10 mostly under-captured by this dataset when compared to the IMD. The WFDEI is
11 developed using ERA-Interim reanalysis and bias-corrected using GPCP dataset. Therefore,
12 subdued monsoon rainfall in India which is noted in ERA-Interim (Kim et al., 2019) may
13 explain this underestimation.

14 The reanalysis datasets showed the largest discrepancies among other precipitation
15 products when compared with the IMD dataset. Overestimation of extreme rainfall over the
16 GP in JRA-55 may be due to the spin-down problem, which simulates excessive
17 precipitation at the start at the forecast (Kobayashi et al., 2015). The PGF reanalysis highly
18 overestimated CWD, and underestimated CDD in India, which may be due to the presence
19 of too little wet days in the dataset. Performance of MERRA-2 is comparatively better than
20 the JRA-55 reanalysis, especially in capturing heavy rainfall amount, frequency of R10mm
21 and CDD in India. Mahato and Mishra et al. 2019 also find similar results while analyzing
22 extreme monsoon season rainfall in India. An improved precipitation correction algorithm
23 and incorporation of merged gauge-satellite data may be the reason for that (Reichle et al.
24 2017). The ERA-5 shows improvements with the sophisticated data assimilation methods
25 and has benefited from improvements in model physics and core development of forecast
26 models (Nogueira, 2020). As discussed above, the difference in grid-resolution also reduces
27 the performance of reanalysis datasets in reproducing extreme precipitation.

28 **5. Conclusion**

29 Understanding extreme rainfall characteristics is crucial as they can have great societal
30 impacts especially under recent warming. Gridded rainfall datasets for studying extreme
31 rainfall are quite an attractive choice as they provide daily precipitation estimates at a high

1 spatial resolution over most parts of the globe. However, their performance must be
2 assessed first before using in hydro-climatological studies. Twelve such daily gridded
3 rainfall datasets from four different sources (comprising gauge-based, satellite, reanalysis,
4 and merged products) are compared with a high-resolution regional dataset from IMD. The
5 paper has the following objectives. First, to assess the spatio-temporal representation of
6 different frequency, magnitude, and duration based extreme rainfall events in these
7 datasets across India. Second, to assess the performance of these datasets in reproducing
8 the spatial pattern of observed trends in frequency, duration, and magnitude based extreme
9 rainfall indices. Third, to identify better performing datasets among the selected ones for
10 extreme rainfall studies in India. The main findings are as follows:

11 Spatially higher extreme rainfall indices (e.g. RX1day, RX5day) are mostly underestimated
12 by these datasets. The amount of dry bias is relatively high for higher extreme indices that
13 are located further into the tail of the daily rainfall distribution (e.g. RX1day and R99tp).
14 The amount of wet bias increases for moderate and lower rainfall extremes (e.g. R20mm
15 and R10mm) as frequency of these indices is overestimated in most parts of India. It is also
16 found that the amount of bias in estimating extreme rainfall is relatively higher over
17 complex topography e.g. Western Ghats, Himalaya, and NE India. Besides, a consistent
18 overestimation of extreme rainfall in the dry parts of Southern Peninsula (leeward side of
19 Western Ghats) is noted in PERSIANN-CDR and JRA-55 over the NW India. The inter-
20 product spread is lower among the gauge-based products and it is highest for reanalysis.
21 However, the ERA-5 reanalysis captures the spatio-temporal variability of extreme rainfall
22 indices better than other reanalyses and even sometimes outperforms other product types
23 (e.g. CPC, WFDEI). Duration-based extreme indices are better captured by the gauge-based
24 datasets than other data types. Due to overestimation of very low rainfall days, CWD is
25 overestimated in these data products. In contrast, the CDD are better captured than CWD.
26 The gauge-based, satellite, and merged products better capture the spatial and temporal
27 variation in dry days.

28 Trends in extreme rainfall indices are quite patchy and found in isolated places in the IMD
29 dataset. This inhomogeneous trend pattern can also be noted in other datasets, although,
30 with some notable exception like the PERSIANN-CDR shows strong drying trend for almost

1 all the extreme indices. In contrast, the CPC and MERRA-2 have wetting trend over India
2 across all the extreme indices, which is in large contrast to the IMD dataset.

3 The study finds that the gauge based GPCC better captures extreme rainfall in India than
4 other datasets. In the satellite-reanalysis group, CHIRPS, and ERA-5 outperformed other
5 datasets, respectively. It is interesting to note that the MSWEP merged datasets is in
6 better agreement with IMD than the satellite reanalysis products. However, there is less
7 consistency among the datasets in estimating trends in extreme rainfall indices over India.
8 Although, regional wetting (EP and western India) and drying trend (GP and NE India)
9 trend patterns are consistent in most of the datasets.

10 Moreover, some of the gridded datasets used in this study are often used to validate global
11 and regional climate models for climate change impact assessment studies and the
12 underestimation of extreme rainfall, which is inherent in these datasets, may introduce
13 larger uncertainties in climate change studies, especially those with an emphasis on
14 extreme precipitation. Therefore, we argue that assessment ability to capture extreme
15 rainfall by gridded datasets over the region of interest is a prerequisite before conducting
16 any research on changing pattern of regional rainfall characteristics in a warming world.

17

18 **Author contributions**

19 **Suman Bhattacharyya:** Conceptualization, Methodology, Data curation, Formal analysis,
20 Visualization, Writing- original draft. **S Sreelesh:** Conceptualization, methodology,
21 Supervision, Writing- Review & Editing. **Andrew King:** Writing- Review & Editing

22 **Acknowledgements**

23 The first author is thankful to the University Grant Commission (UGC), Government of
24 India for providing financial assistance under the Junior Research Fellowship (UGC-NET-
25 JRF) scheme. Third author received funding from the Australian Research Council
26 (DE180100638). We also acknowledge anonymous reviewer for the constructive suggestions
27 provided to improve.

28 **References**

1 Alexander, L.V., Bador, M., Roca, R., Contractor, S., Donat, M.G. and Nguyen, P.L., 2020.
2 Intercomparison of annual precipitation indices and extremes over global land areas from
3 in situ, space-based and reanalysis products. *Environ. Res. Lett.*, 15(5), p.055002.
4 <https://doi.org/10.1088/1748-9326/ab79e2>

5 Ahmed, K., Shahid, S., Wang, X., Nawaz, N. and Khan, N., 2019. Evaluation of gridded
6 precipitation datasets over arid regions of Pakistan. *Water*, 11(2), p.210.
7 <https://doi.org/10.3390/w11020210>

8 Ashouri, H., Hsu, K.L., Sorooshian, S., Braithwaite, D.K., Knapp, K.R., Cecil, L.D., Nelson,
9 B.R. and Prat, O.P., 2015. PERSIANN-CDR: Daily precipitation climate data record from
10 multisatellite observations for hydrological and climate studies. *Bull Am Meteorol Soc*,
11 96(1), pp.69-83. <https://doi.org/10.1175/BAMS-D-13-00068.1>

12 Avila, F.B., Dong, S., Menang, K.P., Rajczak, J., Renom, M., Donat, M.G. and Alexander,
13 L.V., 2015. Systematic investigation of gridding-related scaling effects on annual statistics
14 of daily temperature and precipitation maxima: A case study for south-east Australia.
15 *Weather and Climate Extremes*, 9, pp.6-16. <https://doi.org/10.1016/j.wace.2015.06.003>

16 Bador, M., Alexander, L.V., Contractor, S. and Roca, R., 2020. Diverse estimates of annual
17 maxima daily precipitation in 22 state-of-the-art quasi-global land observation
18 datasets. *Environ. Res. Lett.*, 15(3), p.035005. <https://doi.org/10.1088/1748-9326/ab6a22>

19 Bai, Xiaoyan, Wen Shen, Xiaoqing Wu, and Peng Wang. "Applicability of long-term
20 satellite-based precipitation products for drought indices considering global warming."
21 *Journal of Environmental Management* 255 (2020): 109846.
22 <https://doi.org/10.1016/j.jenvman.2019.109846>

23 Beck, H.E., Vergopolan, N., Pan, M., Levizzani, V., Van Dijk, A.I., Weedon, G.P., Brocca, L.,
24 Pappenberger, F., Huffman, G.J. and Wood, E.F., 2017. Global-scale evaluation of 22
25 precipitation datasets using gauge observations and hydrological modeling. *Hydrology and*
26 *Earth System Sciences*, 21(12), pp.6201-6217. <https://doi.org/10.5194/hess-21-6201-2017>

27 Beck, H.E., Wood, E.F., Pan, M., Fisher, C.K., Miralles, D.G., Van Dijk, A.I., McVicar, T.R.
28 and Adler, R.F., 2019. MSWEP V2 global 3-hourly 0.1 precipitation: methodology and

1 quantitative assessment. Bulletin of the American Meteorological Society, 100(3), pp.473-
2 500. <https://doi.org/10.1175/BAMS-D-17-0138.1>

3 Belo-Pereira, M., Dutra, E. and Viterbo, P., 2011. Evaluation of global precipitation data
4 sets over the Iberian Peninsula. J. Geophys. Res. Atmos., 116(D20).
5 <https://doi.org/10.1029/2010JD015481>

6 Bharti, V., Singh, C., Ettema, J. and Turkington, T.A.R., 2016. Spatiotemporal
7 characteristics of extreme rainfall events over the Northwest Himalaya using satellite
8 data. Int J Climatol, 36(12), pp.3949-3962. <https://doi.org/10.1002/joc.4605>

9 Bhattacharyya, S. and Sanyal, J., 2019. Impact of different types of meteorological data
10 inputs on predicted hydrological and erosive responses to projected land use changes. J.
11 Earth Syst. Sci., 128(3), p.60. <https://doi.org/10.1007/s12040-019-1076-y>

12 Cavalcante, R.B.L., da Silva Ferreira, D.B., Pontes, P.R.M., Tedeschi, R.G., da Costa,
13 C.P.W. and de Souza, E.B., 2020. Evaluation of extreme rainfall indices from CHIRPS
14 precipitation estimates over the Brazilian Amazonia. Atmos Res, 238, p.104879.
15 <https://doi.org/10.1016/j.atmosres.2020.104879>

16 Chaudhary, S., Dhanya, C.T. and Vinnarasi, R., 2017. Dry and wet spell variability during
17 monsoon in gauge-based gridded daily precipitation datasets in India. J. Hydrol., 546,
18 pp.204-218. <https://doi.org/10.1016/j.jhydrol.2017.01.023>

19 Chen, M., Shi, W., Xie, P., Silva, V.B., Kousky, V.E., Wayne Higgins, R. and Janowiak, J.E.,
20 2008. Assessing objective techniques for gauge-based analyses of global daily precipitation.
21 J. Geophys. Res. Atmos., 113(D4). <https://doi.org/10.1029/2007JD009132>

22 Chen, S., Gan, T.Y., Tan, X., Shao, D. and Zhu, J., 2019. Assessment of CFSR, ERA-
23 Interim, JRA-55, MERRA-2, NCEP-2 reanalysis data for drought analysis over
24 China. Clim. Dyn., 53(1-2), pp.737-757. <https://doi.org/10.1007/s00382-018-04611-1>

25 Chen, S., Liu, B., Tan, X., Wu, Y. (2020). Inter-comparison of spatiotemporal features of
26 precipitation extremes within six daily precipitation products. Clim. Dyn., 54, pp. 1057–
27 1076 <https://doi.org/10.1007/s00382-019-05045-z>

1 Contractor, S., Donat, M.G., Alexander, L.V., Ziese, M., Meyer-Christoffer, A., Schneider,
2 U., Rustemeier, E., Becker, A., Durre, I. and Vose, R.S., 2020. Rainfall Estimates on a
3 Gridded Network (REGEN)—a global land-based gridded dataset of daily precipitation from
4 1950 to 2016. *Hydrology and Earth System Sciences*, 24(2), pp.919-943.
5 <https://doi.org/10.5194/hess-24-919-2020>

6 Dash, S. and Maity, R., 2019. Temporal evolution of precipitation-based climate change
7 indices across India: contrast between pre-and post-1975 features. *Theor. Appl. Climatol.*,
8 138(3-4), pp.1667-1678. <https://doi.org/10.1007/s00704-019-02923-8>

9 Dee, D.P., Uppala, S.M., Simmons, A.J., Berrisford, P., Poli, P., Kobayashi, S., Andrae, U.,
10 Balmaseda, M.A., Balsamo, G., Bauer, D.P. and Bechtold, P., 2011. The ERA-Interim
11 reanalysis: Configuration and performance of the data assimilation system. *Q J R Meteorol*
12 *Soc*, 137(656), pp.553-597. <https://doi.org/10.1002/qj.828>

13 Essou, G.R., Sabarly, F., Lucas-Picher, P., Brissette, F. and Poulin, A., 2016. Can
14 precipitation and temperature from meteorological reanalyses be used for hydrological
15 modeling?. *Journal of Hydrometeorology*, 17(7), pp.1929-1950. [https://doi.org/10.1175/JHM-](https://doi.org/10.1175/JHM-D-15-0138.1)
16 [D-15-0138.1](https://doi.org/10.1175/JHM-D-15-0138.1)

17 Fallah, A., Rakhshandehroo, G.R., Berg, P., O, S. and Orth, R., 2019. Evaluation of
18 precipitation datasets against local observations in Southwestern Iran. *Int J Climatol.*
19 <https://doi.org/10.1002/joc.6445>

20 Fischer, E.M. and Knutti, R., 2015. Anthropogenic contribution to global occurrence of
21 heavy-precipitation and high-temperature extremes. *Nat Clim Chang*, 5(6), pp.560-564.
22 <https://doi.org/10.1038/nclimate2617>

23 Funk, C., Peterson, P., Landsfeld, M., Pedreros, D., Verdin, J., Shukla, S., Husak, G.,
24 Rowland, J., Harrison, L., Hoell, A. and Michaelsen, J., 2015. The climate hazards infrared
25 precipitation with stations—a new environmental record for monitoring extremes. *Sci.*
26 *Data*, 2(1), pp.1-21. <https://doi.org/10.1038/sdata.2015.66>

27 Gao, F., Zhang, Y., Chen, Q., Wang, P., Yang, H., Yao, Y. and Cai, W., 2018. Comparison of
28 two long-term and high-resolution satellite precipitation datasets in Xinjiang, China.
29 *Atmospheric Research*, 212, pp.150-157. <https://doi.org/10.1016/j.atmosres.2018.05.016>

1 Gelaro, R., McCarty, W., Suárez, M.J., Todling, R., Molod, A., Takacs, L., Randles, C.A.,
2 Darnenov, A., Bosilovich, M.G., Reichle, R. and Wargan, K., 2017. The modern-era
3 retrospective analysis for research and applications, version 2 (MERRA-2). *J. Clim.*, 30(14),
4 pp.5419-5454. <https://doi.org/10.1175/JCLI-D-16-0758.1>

5 Gervais, M., Tremblay, L.B., Gyakum, J.R. and Atallah, E., 2014. Representing extremes in
6 a daily gridded precipitation analysis over the United States: Impacts of station density,
7 resolution, and gridding methods. *J. Clim.*, 27(14), pp.5201-5218.
8 <https://doi.org/10.1175/JCLI-D-13-00319.1>

9 Gilmont, M., Hall, J.W., Grey, D., Dadson, S.J., Abele, S. and Simpson, M., 2018. Analysis
10 of the relationship between rainfall and economic growth in Indian states. *Glob Environ*
11 *Change*, 49, pp.56-72. <https://doi.org/10.1016/j.gloenvcha.2018.01.003>

12 Ghodichore, N., Vinnarasi, R., Dhanya, C.T. and Roy, S.B., 2018. Reliability of reanalyses
13 products in simulating precipitation and temperature characteristics in India. *J. Earth*
14 *Syst. Sci.*, 127(8), p.115. <https://doi.org/10.1007/s12040-018-1024-2>

15 Golian, S., Javadian, M. and Behrangi, A., 2019. On the use of satellite, gauge, and
16 reanalysis precipitation products for drought studies. *Environ. Res. Lett.*, 14(7), p.075005.
17 <https://doi.org/10.1088/1748-9326/ab2203>

18 Goswami, B.N., Venugopal, V., Sengupta, D., Madhusoodanan, M.S. and Xavier, P.K., 2006.
19 Increasing trend of extreme rain events in India in a warming environment. *Science*,
20 314(5804), pp.1442-1445. <https://doi.org/10.1126/science.1132027>

21 Gupta, V., Jain, M.K., Singh, P.K. and Singh, V., 2019. An assessment of global satellite-
22 based precipitation datasets in capturing precipitation extremes: A comparison with
23 observed precipitation dataset in India. *Int J Climatol.* <https://doi.org/10.1002/joc.6419>

24 Gupta, V. and Jain, M.K., 2020. Impact of ENSO, global warming, and land surface
25 elevation on extreme precipitation in India. *J Hydrol Eng*, 25(1), p.05019032.
26 [https://doi.org/10.1061/\(ASCE\)HE.1943-5584.0001872](https://doi.org/10.1061/(ASCE)HE.1943-5584.0001872)

1 Herold, N., Behrangi, A. and Alexander, L.V., 2017. Large uncertainties in observed daily
2 precipitation extremes over land. *J. Geophys. Res. Atmos.*, 122(2), pp.668-681.
3 <https://doi.org/10.1002/2016JD025842>

4 Hersbach, H., Bell, B., Berrisford, P., Hirahara, S., Horányi, A., Muñoz-Sabater, J., Nicolas,
5 J., Peubey, C., Radu, R., Schepers, D. and Simmons, A., 2020. The ERA5 global reanalysis.
6 *Q J R Meteorol Soc*, 146(730), pp.1999-2049. <https://doi.org/10.1002/qj.3803>

7 Huang, D.Q., Zhu, J., Zhang, Y.C., Huang, Y. and Kuang, X.Y., 2016. Assessment of
8 summer monsoon precipitation derived from five reanalysis datasets over East Asia. *Q J R*
9 *Meteorol Soc*, 142(694), pp.108-119. <https://doi.org/10.1002/qj.2634>

10 India Meteorological Department. 2015. Forecasters' Guide. (Forecasting Circular
11 No. 5/2015 (3.7)).

12

13 IPCC, 2014. Climate Change 2014: Synthesis Report. Contribution of Working Groups I, II
14 and III to the Fifth Assessment Report of the Intergovernmental Panel on Climate Change.
15 [Core Writing Team, R.K. Pachauri and L.A. Meyer (eds.)]. IPCC, Geneva, Switzerland,
16 p151.

17 Jena, P., Garg, S. and Azad, S., 2020. Performance Analysis of IMD High-Resolution
18 Gridded Rainfall (0.25°× 0.25°) and Satellite Estimates for Detecting Cloudburst Events
19 over the Northwest Himalayas. *Journal of Hydrometeorology*, 21(7), pp.1549-1569.
20 <https://doi.org/10.1175/JHM-D-19-0287.1>

21 Kanamitsu, M., Ebisuzaki, W., Woollen, J., Yang, S.K., Hnilo, J.J., Fiorino, M. and Potter,
22 G.L., 2002. Ncep–doe amip-ii reanalysis (r-2). *Bull Am Meteorol Soc*, 83(11), pp.1631-1644.
23 <https://doi.org/10.1175/BAMS-83-11-1631>

24 Kendall, M.G., 1975. Rank correlation methods, 4th ed. Charles Griffin, London, 202

25 Kidd, C., Becker, A., Huffman, G.J., Muller, C.L., Joe, P., Skofronick-Jackson, G. and
26 Kirschbaum, D.B., 2017. So, how much of the Earth's surface is covered by rain
27 gauges?. *Bull Am Meteorol Soc*, 98(1), pp.69-78. [http://dx.doi.org/10.1175/BAMS-D-14-](http://dx.doi.org/10.1175/BAMS-D-14-00283.1)
28 [00283.1](http://dx.doi.org/10.1175/BAMS-D-14-00283.1)

1 Kim, I.W., Oh, J., Woo, S. and Kripalani, R.H., 2019. Evaluation of precipitation extremes
2 over the Asian domain: observation and modelling studies. *Clim. Dyn.*, 52(3-4), pp.1317-
3 1342. <https://doi.org/10.1007/s00382-018-4193-4>

4 Kim, Y.H., Min, S.K., Zhang, X., Sillmann, J. and Sandstad, M., 2020. Evaluation of the
5 CMIP6 multi-model ensemble for climate extreme indices. *Weather. Clim. Extremes*, 29,
6 p.100269. <https://doi.org/10.1016/j.wace.2020.100269>

7 King, A.D., Alexander, L.V. and Donat, M.G., 2013. The efficacy of using gridded data to
8 examine extreme rainfall characteristics: a case study for Australia. *Int J Climatol*, 33(10),
9 pp.2376-2387. <https://doi.org/10.1002/joc.3588>

10 Kobayashi, S., Ota, Y., Harada, Y., Ebata, A., Moriya, M., Onoda, H., Onogi, K., Kamahori,
11 H., Kobayashi, C., Endo, H. and Miyaoka, K., 2015. The JRA-55 reanalysis: General
12 specifications and basic characteristics. *J. Meteorol. Soc. Japan. Ser. II*, 93(1), pp.5-48.
13 <https://doi.org/10.2151/jmsj.2015-001>

14 Kolluru, V., Kolluru, S. and Konkathi, P., 2020. Evaluation and integration of reanalysis
15 rainfall products under contrasting climatic conditions in India. *Atmos Res*, 246, p.105121.
16 <https://doi.org/10.1016/j.atmosres.2020.105121>

17 Kursinski, A.L. and Zeng, X., 2006. Areal estimation of intensity and frequency of
18 summertime precipitation over a midlatitude region. *Geophys. Res. Lett.*, 33(22).
19 <https://doi.org/10.1029/2006GL027393>

20 Mahto, S.S. and Mishra, V., 2019. Does ERA-5 outperform other reanalysis products for
21 hydrologic applications in India?. *J. Geophys. Res. Atmos.*, 124(16), pp.9423-9441.
22 <https://doi.org/10.1029/2019JD031155>

23 Mann, H.B., 1945. Nonparametric tests against trend. *Econometrica: Journal of the*
24 *Econometric Society*, pp.245-259

25 Matthews, T., Wilby, R.L. and Murphy, C., 2019. An emerging tropical cyclone–deadly heat
26 compound hazard. *Nat Clim Chang*, 9(8), pp.602-606. <https://doi.org/10.1038/s41558-019-0525-6>
27

1 Masunaga, H., Schröder, M., Furuzawa, F.A., Kummerow, C., Rustemeier, E. and
2 Schneider, U., 2019. Inter-product biases in global precipitation extremes. *Environ. Res.*
3 *Let.*, 14(12), p.125016. <https://doi.org/10.1088/1748-9326/ab5da9>

4 Mondal, A., Lakshmi, V. and Hashemi, H., 2018. Intercomparison of trend analysis of
5 multisatellite monthly precipitation products and gauge measurements for river basins of
6 India. *J. Hydrol.*, 565, pp.779-790. <https://doi.org/10.1016/j.jhydrol.2018.08.083>

7 Moriasi, D.N., Arnold, J.G., Van Liew, M.W., Bingner, R.L., Harmel, R.D. and Veith, T.L.,
8 2007. Model evaluation guidelines for systematic quantification of accuracy in watershed
9 simulations. *Trans ASABE*, 50(3), pp.885-900. doi: 10.13031/2013.23153

10 Nguyen, P., Ombadi, M., Sorooshian, S., Hsu, K., AghaKouchak, A., Braithwaite, D.,
11 Ashouri, H. and Thorstensen, A.R., 2018. The PERSIANN family of global satellite
12 precipitation data: A review and evaluation of products. *Hydrol Earth Syst Sci*22(11),
13 pp.5801-5816. <https://doi.org/10.5194/hess-22-5801-2018>

14 Nogueira, M., 2020. Inter-comparison of ERA-5, ERA-interim and GPCP rainfall over the
15 last 40 years: Process-based analysis of systematic and random differences. *J. Hydrol.*, 583,
16 p.124632. <https://doi.org/10.1016/j.jhydrol.2020.124632>

17 Pai, D.S., Sridhar, L., Rajeevan, M., Sreejith, O.P., Satbhai, N.S. and Mukhopadhyay, B.,
18 2014. Development of a new high spatial resolution (0.25× 0.25) long period (1901–2010)
19 daily gridded rainfall data set in India and its comparison with existing data sets over the
20 region. *Mausam*, 65(1), pp.1-18.

21 Pai, D.S., Sridhar, L., Badwaik, M.R. and Rajeevan, M., 2015. Analysis of the daily rainfall
22 events in India using a new long period (1901–2010) high resolution (0.25× 0.25) gridded
23 rainfall data set. *Clim. Dyn.*, 45(3), pp.755-776. <https://doi.org/10.1007/s00382-014-2307-1>

24 Paik, S., Min, S.K., Zhang, X., Donat, M.G., King, A.D. and Sun, Q., 2020. Determining the
25 anthropogenic greenhouse gas contribution to the observed intensification of extreme
26 precipitation. *Geophys. Res. Lett.*, 47(12), p.e2019GL086875.
27 <https://doi.org/10.1029/2019GL086875>

1 Pattanaik, D.R. and Rajeevan, M., 2010. Variability of extreme rainfall events in India
2 during southwest monsoon season. Meteorol. Appl., 17(1), pp.88-104.
3 <https://doi.org/10.1002/met.164>

4 Perkins-Kirkpatrick, S.E. and Lewis, S.C., 2020. Increasing trends in regional heatwaves.
5 Nat. Commun., 11(1), pp.1-8. <https://doi.org/10.1038/s41467-020-16970-7>

6 Pradhan, R.K., Sharma, D., Panda, S.K., Dubey, S.K. and Sharma, A., 2019. Changes of
7 precipitation regime and its indices over Rajasthan state of India: impact of climate change
8 scenarios experiments. Clim. Dyn., 52(5-6), pp.3405-3420. [https://doi.org/10.1007/s00382-](https://doi.org/10.1007/s00382-018-4334-9)
9 [018-4334-9](https://doi.org/10.1007/s00382-018-4334-9)

10 Prakash, S., 2019. Performance assessment of CHIRPS, MSWEP, SM2RAIN-CCI, and
11 TMPA precipitation products across India. J. Hydrol., 571, pp.50-59.
12 <https://doi.org/10.1016/j.jhydrol.2019.01.036>

13 Rai, P.K., Singh, G.P. and Dash, S.K., 2020. Projected changes in extreme precipitation
14 events over various subdivisions of India using RegCM4. Clim. Dyn., 54(1-2), pp.247-272.
15 <https://doi.org/10.1007/s00382-019-04997-6>

16 Rajeevan, M., Bhate, J. and Jaswal, A.K., 2008. Analysis of variability and trends of
17 extreme rainfall events in India using 104 years of gridded daily rainfall data. Geophys.
18 Res. Lett., 35(18). <https://doi.org/10.1029/2008GL035143>

19 Rajeevan, M. and Bhate, J., 2009. A high resolution daily gridded rainfall dataset (1971–
20 2005) for mesoscale meteorological studies. Current Science, pp.558-562.

21 Rajulapati, C.R., Papalexiou, S.M., Clark, M.P., Razavi, S., Tang, G. and Pomeroy, J.W.,
22 2020. Assessment of extremes in global precipitation products: How reliable are they?.
23 Journal of Hydrometeorology, 21(12), pp.2855-2873. [https://doi.org/10.1175/JHM-D-20-](https://doi.org/10.1175/JHM-D-20-0040.1)
24 [0040.1](https://doi.org/10.1175/JHM-D-20-0040.1)

25 Rana, S., McGregor, J. and Renwick, J., 2015. Precipitation seasonality over the Indian
26 subcontinent: An evaluation of gauge, reanalyses, and satellite retrievals. J
27 Hydrometeorol 16(2), pp.631-651. <https://doi.org/10.1175/JHM-D-14-0106.1>

1 Reichle, R.H., Liu, Q., Koster, R.D., Draper, C.S., Mahanama, S.P. and Partyka, G.S., 2017.
2 Land surface precipitation in MERRA-2. *J. Clim.*, 30(5), pp.1643-1664.
3 <https://doi.org/10.1175/JCLI-D-16-0570.1>

4 Roca, R., Alexander, L.V., Potter, G., Bador, M., Jucá, R., Contractor, S., Bosilovich, M.G.
5 and Cloché, S., 2019. FROGS: a daily 1°× 1° gridded precipitation database of rain gauge,
6 satellite and reanalysis products. *Earth System Science Data*, 11(3), pp.1017-1035.
7 <https://doi.org/10.5194/essd-11-1017-2019>

8 Salman, S.A., Shahid, S., Ismail, T., Al-Abadi, A.M., Wang, X.J. and Chung, E.S., 2019.
9 Selection of gridded precipitation data for Iraq using compromise programming.
10 *Measurement*, 132, pp.87-98. <https://doi.org/10.1016/j.measurement.2018.09.047>

11 Santos, C.A.G., Neto, R.M.B., do Nascimento, T.V.M., da Silva, R.M., Mishra, M. and Frade,
12 T.G., 2021. Geospatial drought severity analysis based on PERSIANN-CDR-estimated
13 rainfall data for Odisha state in India (1983–2018). *Science of The Total Environment*, 750,
14 p.141258. <https://doi.org/10.1016/j.scitotenv.2020.141258>

15 Satgé, F., Defrance, D., Sultan, B., Bonnet, M.P., Seyler, F., Rouché, N., Pierron, F. and
16 Paturel, J.E., 2020. Evaluation of 23 gridded precipitation datasets across West Africa. *J.*
17 *Hydrol.*, 581, p.124412. <https://doi.org/10.1016/j.jhydrol.2019.124412>

18 Schamm, K., Ziese, M., Becker, A., Finger, P., Meyer-Christoffer, A., Schneider, U.,
19 Schröder, M. and Stender, P., 2014. Global gridded precipitation over land: a description of
20 the new GPCP First Guess Daily product. *Earth Syst. Sci. Data*, 6(1), p.49.
21 <https://doi.org/10.5194/essd-6-49-2014>

22 Schneider, U., Becker, A., Finger, P., Meyer-Christoffer, A., Ziese, M. and Rudolf, B., 2014.
23 GPCP's new land surface precipitation climatology based on quality-controlled in situ data
24 and its role in quantifying the global water cycle. *Theor. Appl. Climatol.*, 115(1-2), pp.15-40.
25 <https://doi.org/10.1007/s00704-013-0860-x>

26 Schoof, J.T. and Robeson, S.M., 2016. Projecting changes in regional temperature and
27 precipitation extremes in the United States. *Weather. Clim. Extremes*, 11, pp.28-40.
28 <https://doi.org/10.1016/j.wace.2015.09.004>

- 1 Sen, P.K., 1968. Estimates of the regression coefficient based on Kendall's tau. J. Am. Stat.
2 Assoc., 63(324), 1379-1389.
- 3 Sharma, A. and Goyal, M.K., 2020. Assessment of the changes in precipitation and
4 temperature in Teesta River basin in Indian Himalayan Region under climate change.
5 Atmos Res, 231, p.104670. <https://doi.org/10.1016/j.atmosres.2019.104670>
- 6 Sheffield, J., Goteti, G. and Wood, E.F., 2006. Development of a 50-year high-resolution
7 global dataset of meteorological forcings for land surface modeling. J. Clim., 19(13),
8 pp.3088-3111. <https://doi.org/10.1175/JCLI3790.1>
- 9 Singh, A.K., Tripathi, J.N., Singh, K.K., Singh, V. and Sateesh, M., 2019. Comparison of
10 different satellite-derived rainfall products with IMD gridded data in Indian meteorological
11 subdivisions during Indian Summer Monsoon (ISM) 2016 at weekly temporal resolution. J.
12 Hydrol., 575, pp.1371-1379.
13 [https://ui.adsabs.harvard.edu/link_gateway/2019JHyd..575.1371K/doi:10.1016/j.jhydrol.201](https://ui.adsabs.harvard.edu/link_gateway/2019JHyd..575.1371K/doi:10.1016/j.jhydrol.2019.02.016)
14 [9.02.016](https://ui.adsabs.harvard.edu/link_gateway/2019JHyd..575.1371K/doi:10.1016/j.jhydrol.2019.02.016)
- 15 Singh, D., Ghosh, S., Roxy, M.K. and McDermid, S., 2019. Indian summer monsoon:
16 Extreme events, historical changes, and role of anthropogenic forcings. Wiley
17 Interdisciplinary Reviews: Climate Change, 10(2), p.e571. <https://doi.org/10.1002/wcc.571>
- 18 Srivastava, A., Grotjahn, R. and Ullrich, P.A., 2020. Evaluation of historical CMIP6 model
19 simulations of extreme precipitation over contiguous US regions. Weather. Clim. Extremes,
20 29, p.100268. <https://doi.org/10.1016/j.wace.2020.100268>
- 21 Sun, Q., Miao, C., Duan, Q., Ashouri, H., Sorooshian, S. and Hsu, K.L., 2018. A review of
22 global precipitation data sets: Data sources, estimation, and intercomparisons. Rev.
23 Geophys., 56(1), pp.79-107. <https://doi.org/10.1002/2017RG000574>
- 24 Teegavarapu, R.S., Goly, A. and Obeysekera, J., 2013. Influences of Atlantic multidecadal
25 oscillation phases on spatial and temporal variability of regional precipitation extremes. J.
26 Hydrol., 495, pp.74-93. <https://doi.org/10.1016/j.jhydrol.2013.05.003>

1 Timmermans, B., Wehner, M., Cooley, D., O'Brien, T. and Krishnan, H., 2019. An
2 evaluation of the consistency of extremes in gridded precipitation data sets. *Clim. Dyn.*,
3 52(11), pp.6651-6670. <https://doi.org/10.1007/s00382-018-4537-0>

4 Viney, N.R. and Bates, B.C., 2004. It never rains on Sunday: the prevalence and
5 implications of untagged multi-day rainfall accumulations in the Australian high quality
6 data set. *Int J Climatol*, 24(9), pp.1171-1192. <https://doi.org/10.1002/joc.1053>

7 Weedon, G.P., Balsamo, G., Bellouin, N., Gomes, S., Best, M.J. and Viterbo, P., 2014. The
8 WFDEI meteorological forcing data set: WATCH Forcing Data methodology applied to
9 ERA-Interim reanalysis data. *Water Resources Research*, 50(9), pp.7505-7514.
10 <https://doi.org/10.1002/2014WR015638>

11 Wiel, K.V.D., Kapnick, S.B., Oldenborgh, G.J.V., Whan, K., Philip, S., Vecchi, G.A., Singh,
12 R.K., Arrighi, J. and Cullen, H., 2017. Rapid attribution of the August 2016 flood-inducing
13 extreme precipitation in south Louisiana to climate change. *Hydrol Earth Syst Sci*21(2),
14 pp.897-921. <https://doi.org/10.5194/hess-21-897-2017>

15 Willmott, C.J., Rowe, C.M. and Philpot, W.D., 1985. Small-scale climate maps: A sensitivity
16 analysis of some common assumptions associated with grid-point interpolation and
17 contouring. *The American Cartographer*, 12(1), pp.5-16.
18 <https://doi.org/10.1559/152304085783914686>

19 Xie P, Yatagai A, Chen M, Hayasaka T, Fukushima Y, Liu C. and Yang, S., 2007. A
20 gaugebased analysis of daily precipitation over East Asia. *J. Hydrometeorol.*, 8:607–626.
21 <https://doi.org/10.1175/JHM583.1>

22 Yang, Q., Leung, L.R., Rauscher, S.A., Ringler, T.D. and Taylor, M.A., 2014. Atmospheric
23 moisture budget and spatial resolution dependence of precipitation extremes in aquaplanet
24 simulations. *J. Clim.*, 27(10), pp.3565-3581. <https://doi.org/10.1175/JCLI-D-13-00468.1>

25 Yatagai, A., Kamiguchi, K., Arakawa, O., Hamada, A., Yasutomi, N. and Kitoh, A., 2012.
26 APHRODITE: Constructing a long-term daily gridded precipitation dataset for Asia based
27 on a dense network of rain gauges. *Bull Am Meteorol Soc*, 93(9), pp.1401-1415.
28 <https://doi.org/10.1175/BAMS-D-11-00122.1>

- 1 Zhan, W., Guan, K., Sheffield, J. and Wood, E.F., 2016. Depiction of drought over sub-
2 Saharan Africa using reanalyses precipitation data sets. *J. Geophys. Res. Atmos.*, 121(18),
3 pp.10-555. <https://doi.org/10.1002/2016JD024858>
- 4 Zhang, X., Alexander, L., Hegerl, G.C., Jones, P., Tank, A.K., Peterson, T.C., Trewin, B. and
5 Zwiers, F.W., 2011. Indices for monitoring changes in extremes based on daily temperature
6 and precipitation data. *Wiley Interdiscip. Rev. Clim. Change*, 2(6), pp.851-870.
7 <https://doi.org/10.1002/wcc.147>
- 8 Zhu, J., Huang, D.Q., Yan, P.W., Huang, Y. and Kuang, X.Y., 2017. Can reanalysis datasets
9 describe the persistent temperature and precipitation extremes over China?. *Theor. Appl.*
10 *Climatol.*, 130(1-2), pp.655-671. <https://doi.org/10.1007/s00704-016-1912-9>

11